SEMMELWEIS EGYETEM

DOKTORI ISKOLA

Ph.D. értekezések

3022.

OLÁH CSILLA

Urológia
című program

Programvezető: Dr. Nyirády Péter, egyetemi tanár

Témavezető: Dr. Szarvas Tibor, tudományos munkatárs

Molecular subtypes and single tissue and serum biomarkers for the prediction of platinum sensitivity of muscle-invasive bladder cancer

PhD thesis

Csilla Oláh

Rácz Károly Doctoral School of Clinical Medicine

Semmelweis University

Supervisor: Tibor Szarvas, DSc, Senior researcher

Official reviewers:

Donát Alpár, PhD, Senior researcher

Levente Kuthi, MD, PhD, University lecturer

Head of the Complex Examination Committee:

Csaba Bödör, DSc, University professor

Members of the Examination Committee:

Tamás Beöthe, MD, PhD, Chief physician
Gábor Szabó, MD, PhD, Chief physician

Budapest, 2024

Table of Contents

List of Abbreviations

AC – Adjuvant chemotherapy

Ba/SCC-like – Basal/Squamous cell carcinoma-like molecular subtype

Ba/Sq – Basal/Squamous molecular subtype

BC – Bladder cancer

BCG – *Bacillus Calmette-Guérin*

CIS – *In situ carcinoma*

CSS – Cancer-specific survival

ELISA – Enzyme-Linked Immunosorbent Assay

FFPE – Formalin-fixed and paraffin-embedded

GSC – Genomic subtyping classifier

GU – Genomically unstable molecular subtype

ICI – Immune checkpoint inhibitor

IHC – Immunohistochemistry

LN – Lymph node

Lum – Luminal molecular subtype

LumI – Luminal-infiltrated molecular subtype

LumNS – Luminal non specified molecular subtype

LumP – Luminal-papillary molecular subtype

LumU– Luminal unstable molecular subtype

MDA – MD Anderson Cancer Center

Mes-like – Mesenchymal-like molecular subtype

MIBC – Muscle-invasive bladder cancer

MMP7 – Matrix Metallopeptidase 7

NAC – Neoadjuvant chemotherapy

Ne – Neuronal molecular subtype

Ne-like – Neuroendocrine-like molecular subtype

NMIBC – Non-muscle invasive bladder cancer

OS – Overall survival

qPCR – quantitative polymerase chain reaction

RC – Radical cystectomy

RFS – Recurrence-free survival

Sc/Ne-like – Small-cell/Neuroendocrine-like molecular subtype

SDC1 – Syndecan 1

TCGA – The Cancer Genome Atlas

TUR – Transurethral resection

TURB – Transurethral resection of bladder

UNC – University of North Carolina

Uro-like – Urothelial-like molecular subtype

1. Introduction

Bladder cancer (BC) is a common malignancy worldwide, with 550 000 newly diagnosed cases and 200 000 deaths in 2018. BC is most prevalent in the developed world, including countries in southern and western Europe, and in North America, and occurs three times more frequently in men than in women. Smoking, exposure to certain chemicals, and water contamination are known risk factors for the development of BC (1). In Hungary, based on data from the National Cancer Registry, the number of newly diagnosed BC was 3546 in 2019 (https://onkol.hu/nemzeti-rakregiszter/), with a slightly increased tendency in the last 20 years (Figure 1). In Hungary, BC represents the 8th highest incidence rate and the 9th highest mortality rate among all cancer types (2).

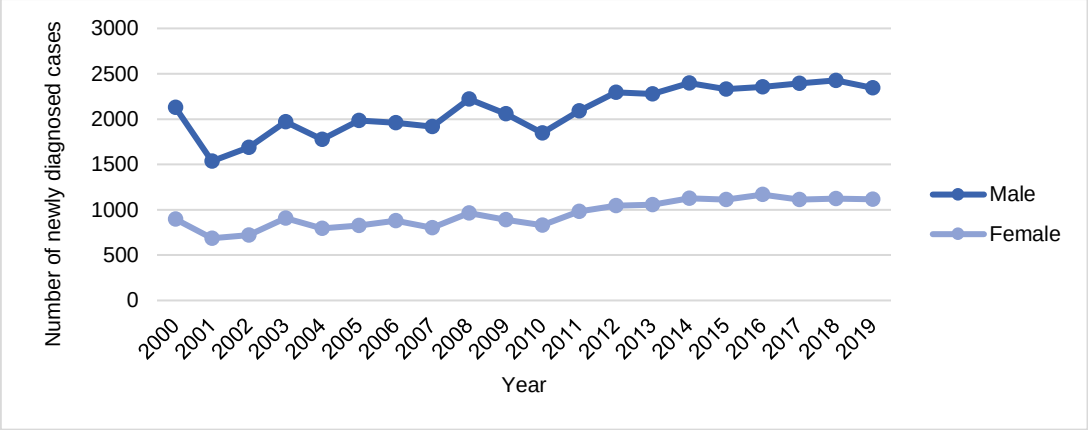

Figure 1. The number of newly diagnosed bladder cancer cases in Hungary between 2000 and 2019.

1.1 Clinical management of BC

The most frequent histological type of BC is urothelial carcinoma. BC can be classified into non-muscle invasive (NMIBC) and muscle-invasive (MIBC) disease, which differ significantly in terms of prognosis and clinical management. Cystoscopy is the gold standard for diagnosing patients with symptoms suggestive of BC, which is most frequently the painless hematuria. The presence of the tumor can then be confirmed by the histological evaluation of transurethral resection (TUR). Approximately 75-80% of newly diagnosed BC cases are NMIBC (≤T1) at first presentation. These patients have a high recurrence rate (60-70%) but a low progression rate to MIBC (15%) and have a good prognosis with over 90% 5-year survival (3, 4).

Patients with NMIBC can be classified into low-, intermediate- and high-risk groups based on the tumor stage, grade, and the presence of *in situ carcinoma* (CIS). A single intravesical instillation of chemotherapy (Mitomycin C, Epirubicin, Pirarubicin) is recommended within 24 hours after TUR for patients with low-risk tumors (Ta, low grade, no CIS, tumor size < 3 cm). Further chemotherapy installation, or *Bacillus Calmette-Guérin* (BCG) treatment is advised for intermediate-risk patients (tumors that are not defined as low or high-risk tumors), and BCG instillation for high-risk patients (high-grade Ta/T1 and/or CIS and/or recurrent tumors). Chemotherapy instillations and BCG therapy proved to reduce the recurrence rate of NMIBCs, however, a life-long cystoscopy surveillance is recommended (3, 5).

The incidence of MIBC represents 20-25% of newly diagnosed cases and its 5-year survival rate is only 50-60%. For patients with muscle-invasive and clinically organ-confined tumors (≥cT2, LN0-LNx, M0) cisplatin-based neoadjuvant chemotherapy (NAC) is the gold standard prior to radical cystectomy (RC) (5). The survival benefit provided by NAC is around 5-8% at 5 years compared to RC alone. On the other hand, the delayed RC due to NAC may reduce the life expectancy for patients with a chemotherapy-resistant tumor (6). Therefore, pre-treatment prediction of platinum sensitivity may help to select patients who benefit from NAC and may help to avoid ineffective platinum treatment and the delay of RC for those who are resistant to NAC.

Adjuvant chemotherapy (AC) is recommended for patients with locally advanced (pT3/4) and/or LN+ tumors at RC, if no NAC has been given preoperatively (7). AC improved overall and disease-specific survival rate with 22% and 34% compared to RC alone according to a meta-analysis with a total of 945 patients (8). Although the guidelines recommending the administration of NAC upfront RC, adjuvant platinum treatment remained still widespread in clinical practice.

There are arguments both for and against NAC and AC therapeutic strategies (9):

Advantages of NAC:

1) NAC is better tolerated than postoperatively applied AC
2) Pathological response rate gives a relatively good estimation on the platinum sensitivity of the tumor.
3) NAC provide an overall survival benefit of 5-8%, which has been confirmed in large prospective studies.

Disadvantages of NAC:

1) Pretreatment staging prior to NAC is based on the transurethral resection of the bladder (TURB) specimen and may therefore be inaccurate.
2) The absolute overall survival benefit is only 5-8%, which is a rather low value.
3) Ineffective NAC delays RC by ~3 months, which may lead to reduced prognosis of patients who are resistant to platinum therapy.

In order to improve the quality of decision-making, chemotherapy predictive markers are needed to identify those patients, who will not benefit from NAC and thereby avoid delayed surgery.

Recently immune checkpoint inhibitor (ICI) therapies, and further novel targeted therapies, such as FGFR inhibitor erdafitinib and two antibody-drug conjugates; the nectin-4 targeting Enfortumab vedotin and the Trop-2 targeting Sacituzumab govitecan have become available as second- and third-line therapies for patients, who had progressed during or following chemotherapy or ICI therapy (10). ICIs are also recommended for cisplatin ineligible and tissue PD-L1 positive patients in first-line setting, and more recently as a maintenance therapy for cisplatin-sensitive patients after response to chemotherapy (11, 12). Figure 2 summarizes the potential therapeutic options of BC patients in detail.

1.2 Platinum predictive biomarkers in BC

The availability of second- and third-line treatments raised an unmet need for clinically available predictive biomarkers, which may help to optimize therapeutic decision-making. Although many efforts have been made to identify predictive biomarkers for chemotherapy, none of the identified markers has been integrated into the clinical practice

yet. Enhanced protein expressions of Emmprin, Survivin, STIP1, HMGA2, and ERCC1 have been shown to be associated with inferior survival in chemotherapy-treated patients. In addition, tumors carrying somatic mutation of *ERCC2*, *ATM*, *RB1*, and *FANCC* showed higher response rates to chemotherapy (13–19) (Table 1).

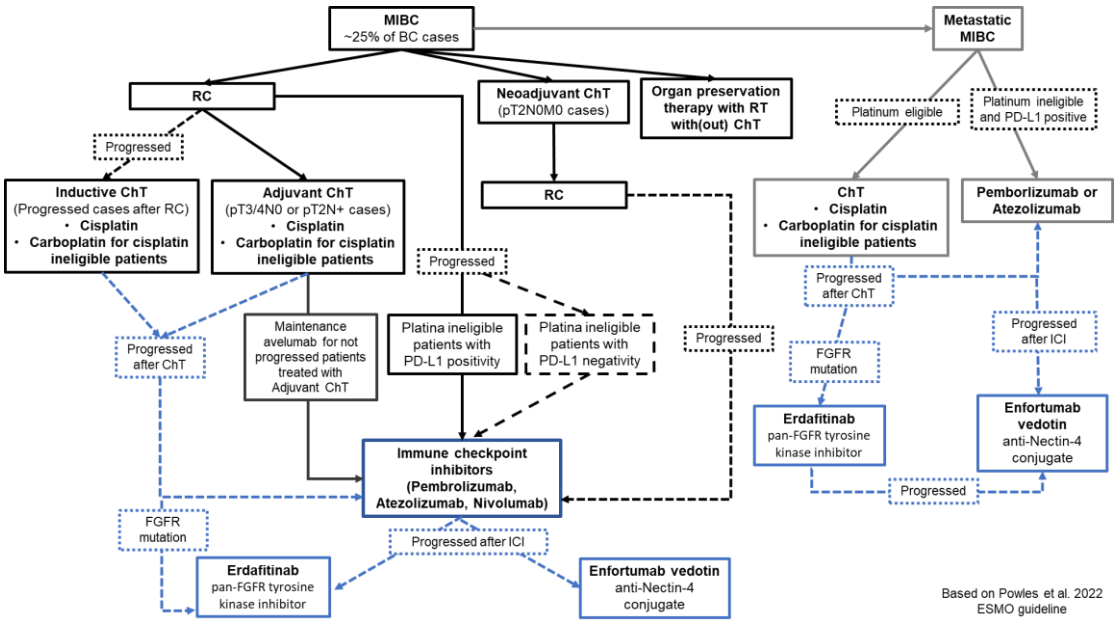

Figure 2. Recommended therapeutic management for patients with BC according to ESMO Clinical Practice Guideline (Powles et al. 2022 (10)). Therapies that could be considered in second-or third-line settings are signed with blue dashed lines. ChT: chemotherapy, MIBC: muscle-invasive bladder cancer, RC: radical cystectomy, RT: radiotherapy.

1.3 Immune checkpoint inhibitor predicting biomarkers in BC

ICI therapies provided a never-before-seen survival benefit in metastatic, platinum-resistant urothelial BC patients. However, only a small rate of ~15-20% BC patients respond to ICI therapy and individual patients may show remarkable differences in their sensitivities to ICIs. Tumor cells proved to be able to escape from cellular immune surveillance by expressing PD-L1 ligands, that are binding to PD-1 receptors of activated T-cells, resulting a blockade in immune response. These immune escape mechanisms can be blocked by the use of anti PD-L1 or anti PD-1 agents (11, 20, 21). PD-L1 immunostaining of tumor and/or immune cells (in terms of TPS, CPS) were shown to be associated with better ICI efficacy and become part of clinical decision-making between carboplatin and ICI for first-line systemic treatment of cisplatin ineligible BC (11, 22). The somatic mutation of *ARID1A* and the higher gene expression of *CXCL13* have been

suggested to be associated with better response and survival rates in ICI treated patients (23) (Table 1).

Table 1. Single predictive markers for the efficacy of chemo- and immune checkpoint inhibitor therapies in muscle-invasive bladder cancer based on literature data. OS: overall survival, PFS: progression-free survival.

Chemotherapy predictive markers

Marker	Impact	Publication	References
Emmprin	positive membrane staining associated with poor outcome	Als et al. 2007	(13)
Survivin	positive cytoplasmatic staining associated with poor outcome	Als et al. 2007	(13)
STIP1	positive nuclear staining associated with worse OS high cytoplasmatic expression associated with shorter PFS	Krafft et al.2019a	(14)
HMGA2	high nuclear staining associated with worse OS	Krafft et al.2019b	(15)
ERCC1	high nuclear expression associated with shorter OS	Ozcan et al. 2012 Sun et al. 2012	(16, 17)
ERCC2	tumors with *ERCC2* somatic mutation responded to chemotherapy	van Allen et al. 2014	(18)
ATM *RB1* *FANCC*	somatic mutation of *ATM* and/or *RB1* and/or *FANCC* are responder to chemotherapy	Plimack et al. 2015	(19)

Immunotherapy predictive markers

Marker	Impact	Publication	Reference
PD-L1	higher expression on immune cells was associated with therapy response and/or longer OS	Rosenberg et al. 2017 Sharma et al. 2017 Powles et al. 2020	(11, 12,20)
ARID1A	somatic mutation of *ARID1A* associated with therapy response and longer OS	Goswami et al. 2020	(23)
CXCL13	higher gene expressions associated with therapy response and longer OS		

1.4 Molecular subtypes in BC

In the last few years, high throughput sequencing and gene expression analyses provided a detailed insight into the molecular background of BC and revealed that histologically similar urothelial BCs have different molecular properties. Several studies have performed mRNA sequencing or gene expression chip analyses and demonstrated that

MIBCs can be classified into various molecular subtypes by using cluster analysis based on gene expression patterns. Subsequent studies demonstrated that distinct molecular subtypes have different prognoses and therapy sensitivity. Early research from the University of North Carolina (UNC) distinguished two well-separated groups; the so-called "luminal" and "basal" subtypes. The luminal subtype shows high gene expression of *KRT19, KRT20, GATA3, FOXA1*, which are typically expressed by the luminal cell layer of the urothelium, while the basal subtype expresses high levels of *KRT5, KRT6, KRT14* genes, which are characteristic for the basal cell layer of the urothelium. These groups proved to be prognostically relevant, as the tumors with luminal gene expression patterns showed prolonged survival compared to basal tumors (24). Later, researchers from the MD Anderson (MDA) Cancer Center distinguished the "p53-like" subtype, which may express both basal and luminal genes but have elevated expression of those genes that are regulated by the p53 expression. The authors also described that patients with a p53-like subtype had less benefit from chemotherapy (25). Considerable attention was subsequently directed to molecular subtypes, and more research groups suggested parallel different but partly overlapping classification systems. The genomic subtyping classifier (GSC) stratified four subtypes, a basal, a luminal, an infiltrated-luminal, and a claudin-low subtype, of which the basal tumors showed improved survival after NAC (26). The Lund classification described two luminal subtypes (urothelial-like and genomically unstable subtypes), a basal subtype, a mesenchymal-like subtype with both low luminal and basal gene expressions, and finally a small-cell/neuroendocrine-like subtype with poor prognosis, which is characterized by high expression of genes which are typically associated with neuroendocrine tumors (27). Later, the same research group comparing BC patients who received NAC before RC and found that only the genomically unstable and urothelial-like tumors benefited from the NAC treatment, while patients with basal subtype did not (28). These results are in contrast with the former findings by *Seiler et al*., who reported that only the basal subtype (by the GSC classifier) benefit from NAC (26). Similar to the Lund classifier, the TCGA (The Cancer Genome Atlas) classifier determined the neuronal subtype in addition to the basal subtype, and three different luminal subtypes (luminal-papillary, luminal-infiltrated, and luminal). The luminal-papillary tumors were found to have the best prognosis, whereas the neuronal subtype was associated with the poorest outcomes (29). The above classification systems

are partly overlapping but do not allow a direct comparison of results between studies using different classifier methods. Therefore, a consensus classification has been suggested based on the reanalysis of 1750 formerly published MIBC transcriptome profiles. This international study agreed to distinguish six Consensus molecular subtypes; (1) luminal papillary, (2) luminal non specified, (3) luminal unstable, (4) stroma-rich, (5) basal, and (6) neuronal-like subtypes. In addition, the study confirmed a better prognosis for luminal papillary, and a poor prognosis for neuronal subtypes, while the authors found no platinum-predictive values of any of the six subtypes. Finally, they suggested that the luminal non specified, luminal unstable, and neuronal-like subtypes could have benefit from ICI therapy (30). Figure 3 illustrates the recently described and partly overlapping molecular subtype classifiers.

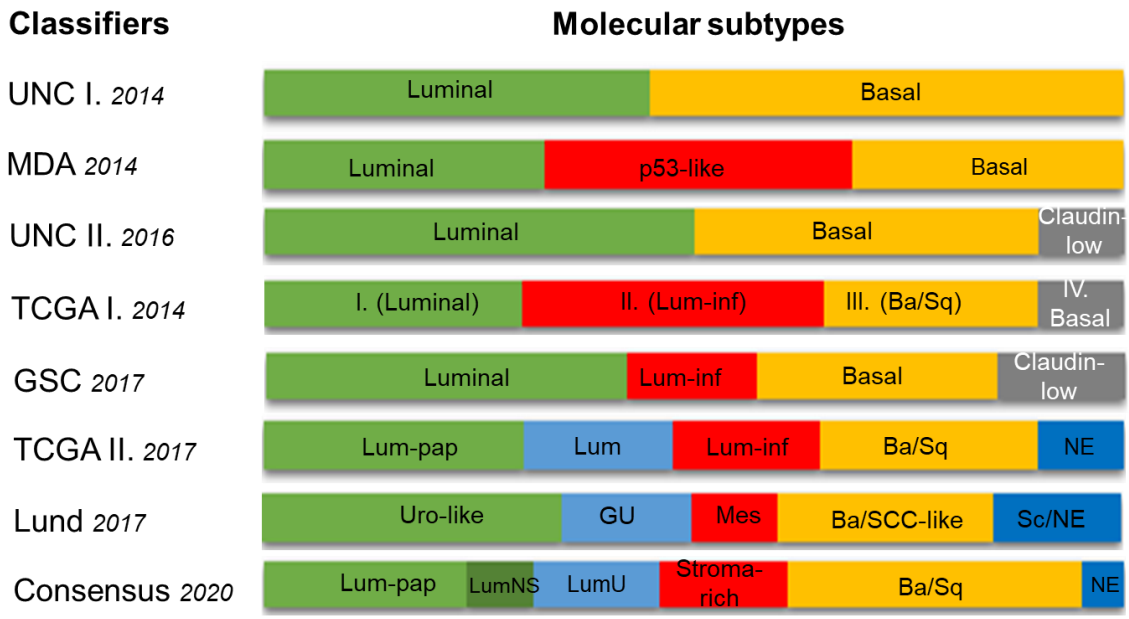

Figure 3. Different molecular classifiers with partly overlapping subtypes. Ba/SCC-like: basal/squamous cell carcinoma, Ba/Sq: basal/squamous, Lum: luminal, Lum-inf: luminal-infiltrated, LumNS: luminal non specified, Lum-pap: luminal-papillary, LumU: luminal unstable, Mes: mesenchymal-like, Ne: neuronal, Sc/Ne: small-cell/neuroendocrine-like, Uro-like: urothelial-like.

Each classifier presented above is based on transcriptome sequencing or gene expression chip data and thus on the analysis of thousands of genes. The molecular classifications had not spread into daily clinical practice yet, due to the methodological complexity and high costs of transcriptome sequencing. Therefore, a simple and cost-effective method is needed to identify molecular subtypes in the everyday practice. A few studies based on

immunohistochemistry (IHC) were published to overcome these methodological difficulties. However, IHC-based approaches typically used only two to five target proteins and can only distinguish luminal, basal, double positive, or double negative subtypes, and therefore cannot reproduce the mRNA-based classification systems (31–33). The only exception is the IHC panel, which was elaborated to reproduce the Lund classification system with five subtypes by using a minimum of 13 protein markers (34). However, the application of 13 IHC markers is still hardly routine compatible.

Taken together, an easily available subtype classifier method is needed, which can be performed on the pathological routine collected formalin-fixed and paraffin-embedded (FFPE) tissue samples and is able to reproduce the most relevant molecular subtype classification systems.

2. Objectives

2.1 The aim of the present retrospective study was:

1) To develop a cost-effective and simple analytical method for the reproduction of the most relevant gene expression-based molecular subtype classification systems.

2) To assess the prognostic and platinum-predictive value of various molecular subtypes in our own institutional BC patient cohorts.

3) To assess the platinum-predictive value of 12 single genes at the mRNA as well as two genes at the protein level in our own institutional BC patient cohorts.

4) To assess the platinum-predictive value of serum markers in our own institutional BC patient cohorts.

Figure 4 outlines the study objectives along with the required steps and measurements essential for accomplishing these aims.

2.2 Required steps / overview of the research

1) Definition of a reduced gene set, which is able to distinguish between various molecular BC subtypes.

2) *In silico* development of classifier methods for each molecular subtype classification systems (MDA, LundTax, TCGA, and Consensus) using the reduced marker set.

3) *In silico* validation of the newly developed classifiers on publicly available datasets.

4) Application of the above developed marker set and classifier methods to our own RC-treated institutional BC cohort. For this, we determined the expression of 68 genes in 100 frozen BC tissue samples by using the TaqMan array card quantitative polymerase chain reaction-based method (qPCR).

5) Application of the above developed (and further improved) marker set and classifier methods to our own institutional cohort of patients with pT3/4 or LN-positive BC, who did *vs*. did not receive adjuvant chemotherapy. For this, we determined the mRNA expression of 48 genes in 160 FFPE tissue samples by the NanoString nCounter method.

6) In addition to subtype-specific genes, we also added 12 single genes with potential platinum-predictive value.

7) Validation of the chemotherapy predictive value of the selected single genes in an independent data set. Two of the 12 markers were also investigated by immunohistochemistry in an independent institutional cohort.

8) Analysis of the chemotherapy predictive value of SDC1 and MMP7 in serum samples by the ELISA method as well as in FFPE tissue samples by immunohistochemistry.

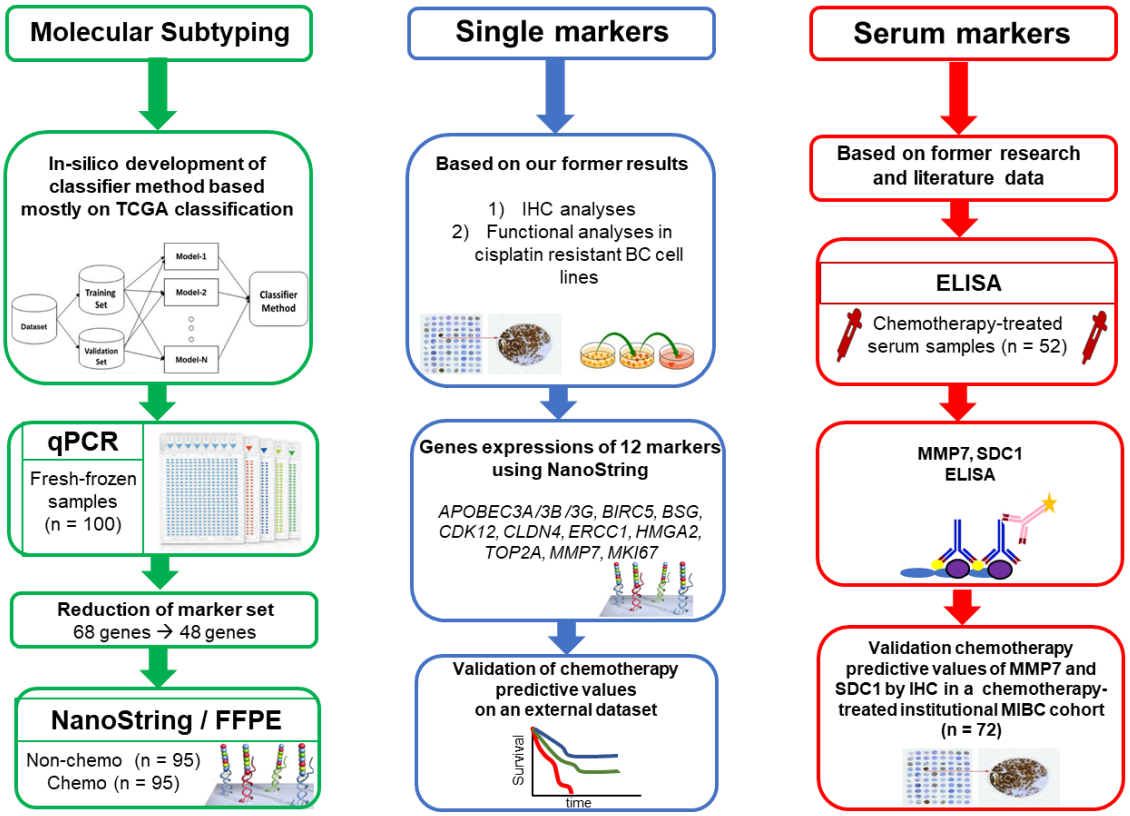

Figure 4. Summary flowchart of the performed analyses. BC: bladder cancer, ELISA: Enzyme-Linked Immunosorbent Assay, FFPE: formalin-fixed and paraffin-embedded, IHC: immunohistochemistry, MIBC: muscle-invasive bladder cancer, qPCR: quantitative polymerase chain reaction, TCGA: The Cancer Genome Atlas.

3. Methods

3.1 Institutional patient cohorts

3.1.1 Frozen bladder cancer tissue cohort for RT-qPCR gene expression analysis

Frozen tumor tissue samples were collected from MIBC patients who underwent RC between 1990 and 2005 at the Department of Urology at the University of Duisburg-Essen. Tissue samples were stained by hematoxylin and eosin and tumorous area were defined by uropathologist. Inclusion criteria were: ≥pT2 urothelial MIBC, no chemotherapy before RC, ≥50% tumor cell content in the tumor tissue, and available follow-up data. Hundred-four samples met the inclusion criteria. Four of 104 samples (4%) were excluded due to lowered gene expression assay (TaqMan) efficiency. Table 2 summarizes the characteristics of 100 patients with fresh-frozen tumor samples, who met the inclusion criteria.

3.1.2 FFPE bladder cancer tissue cohort for NanoString gene expression analysis

FFPE tumor samples were collected from patients with MIBC, who underwent RC between 2005 and 2018 at the Department of Urology, University of Duisburg-Essen and Semmelweis University, Budapest. Inclusion criteria were: ≥pT3 and/or lymph node positivity at RC (indication for an adjuvant platinum-based chemotherapy), no chemotherapy before RC, ≥50% tumor cell content in the tumor tissue, and available follow-up data. Hundred-ninety-one samples met the inclusion criteria. Ninety-five patients received adjuvant platinum-based chemotherapy (chemo cohort) within 90 days after RC, while 96 patients did not receive postoperative chemotherapy (non-chemo cohort). Eight of 191 (4%) samples were excluded due to low gene expression assay (NanoString) efficiency. Further 23 patients with distant metastasis at RC were excluded from final data analysis. Table 4 summarizes the characteristics of 160 patients with FFPE MIBC tumor samples.

3.1.3 FFPE bladder cancer tissue cohort for immunohistochemistry

For IHC analysis, FFPE tumor samples were collected from patients with MIBC, who received postoperative platinum-based chemotherapy between 2004 and 2010 at the Department of Urology, University Hospital of Essen (n = 29) or were enrolled in a phase II, prospective, multicenter, randomized, double-blinded trial (n = 43) (SUSE, AB 31/05, RUTT 204).

3.1.4 Bladder cancer serum samples for ELISA analysis

Baseline serum samples were collected from MIBC patients, who received postoperative platinum-based chemotherapy between 2010 and 2017 at the Department of Urology, University Hospital of Essen (n = 16) and the Department of Urology, Semmelweis University of Budapest (n = 36). Inclusion criteria were: ≥pT2 urothelial MIBC, no chemotherapy before RC. Table 5 summarizes the characteristics of serum and IHC patient cohorts.

3.1.5 Ethics statement

The studies were performed according to the Declaration of Helsinki and the institutional ethics committees approved the study protocols (08-3942-BO /15-6400-BO, TUKEB 55/2014, AB 31/05, RUTT 204).

3.2 RNA extraction and gene expression analyses

RNA was isolated from fresh-frozen RC specimens using RNeasy Kit (Qiagen, Hilden, Germany) according to the manufacturer's protocol. Then, 500 ng RNA was reverse transcribed using the Multiscribe Reverse Transcriptase Kit (Thermo Fisher Scientific, Waltham, MA, USA). Gene expression levels of selected genes (Section 4.1) were measured by TaqMan Gene Expression Assay using the 364-well TaqMan Array Card platform on QuantStudio™ 7 Flex Real-Time PCR System (Applied Biosystems, Life Technologies, Thermo Fisher Scientific, Waltham, MA, USA) according to manufacturer's protocol. The list of determined genes and the detailed evaluation of gene expression results are described in Section 4.1.

RNA was isolated from FFPE RC specimens using RNeasy DSP FFPE Kit (Qiagen, Hilden, Germany) according to the manufacturer's protocol. Prior to RNA extraction, macrodissection has been performed and only the marked tumor areas were used for RNA extraction. Gene expression analysis with a custom gene panel of 48 molecular subtype-specific and 12 additional single genes (Section 4.3) was run on the NanoString nCounter Analysis System (NanoString Technologies, Seattle, WA, USA). For data analysis, the nSolver 4.0 Software was applied. Gene expressions were normalized to the geometric mean of two reference genes (TBP, GAPDH), six internal positive controls, and eight internal negative controls. The list of determined genes and the detailed evaluation of gene expression results are described in Section 4.3.

3.3 Enzyme-Linked Immunosorbent Assay (ELISA)

Patients' baseline SDC1 serum levels were determined by the SDC1 ELISA kit (Diaclone CD138, Gene-Probe, San Diego, CA, USA; Cat. Nr.: 950.640.096) according to the manufacturer's instructions. The cut-off value of SDC1 for dichotomization was set at the upper 25th percentile (180 ng/mL).

Patients' baseline MMP7 serum levels were measured using a Quantikine ELISA kit from R&D Systems (Wiesbaden, Germany; Cat. Nr.: DMP700) according to the manufacturer's instructions. The cut-off value of MMP7 for dichotomization was set at the median.

3.4 Immunohistochemistry

To perform SDC1 IHC staining a mouse monoclonal antibody against SDC1/CD138 (clone MI15, dilution 1:100, Dako/Agilent, Santa Clara, CA, USA) was used after heat-based antigen retrieval (30 min, 96◦C, pH 6.0) on the FFPE sections. SDC1 staining intensity was scored as 1, 2, or 3, equivalent to negative, moderate, and strong intensities. A percentage score was also defined as 0–10%—0 Pts., 11–20%—1 Pt., 21–30%—2 Pts., 31–40%—3 Pts., 41–50%—4 Pts., 51–60%—5 Pts., 61–70%—6 Pts., 71–80%—7 Pts., 81–90%—8 Pts., 91–100%—9 Pts. Then, an IHC-score was calculated by multiplying the intensity score and percentage score. Weak SDC1 expression was considered as a score <4, moderate ≥4 and <10, and strong expression was considered as a score ≥10. SDC1 expression was evaluated separately for cell membrane, cytoplasm, and stroma.

To perform MMP7 IHC staining a mouse monoclonal antibody against MMP7 (JL07, dilution 1:75, Santa Cruz Biotechnology, Dallas, Texas, USA) was used after heat-based antigen retrieval (20 min, 95°C water bath, citrate buffer [pH 6]). MMP7 staining intensity was scored as 1, 2, or 3, equivalent to negative, moderate, and strong intensities, while a percentage score was defined as 0–10%—0 Pts., 11–50%—1 Pts., 51–80% —2 Pts., and 81–100%—3 Pts.. Then, a score was calculated by multiplying the intensity score and percentage score. High MMP7 expression was considered as IHC-score >3.

To perform CLDN4 staining a mouse monoclonal antibody (clone 3e2c1, dilution 1:1000, Invitrogen, Waltham, Massachusetts, USA) was used after heat-based antigen retrieval (24 min, 96◦C, pH 6.0). CLDN4 staining intensity was scored as 1, 2, or 3, equivalent to negative, moderate, and strong intensities. High CLDN4 expression was considered as intensity >1.

To perform ERCC1 staining a mouse monoclonal antibody (Mob 336-05, clone: 8F1, dilution 1:100, Diagnostic Biosystems, CA, USA). ERCC1 staining intensity was scored as 1, 2, or 3, equivalent to negative, moderate, and strong intensities, while a percentage score was defined as 0–10%—0 Pts., 11–50%—1 Pts., 51–80% —2 Pts., and 81–100%—3 Pts.. Then, an IHC-score was calculated by multiplying the intensity score and percentage score. High ERCC1 expression was considered as IHC-score >4.

3.5 Statistical analysis

Chi2 test for the dichotomized variables and Mann-Whitney test for the continuous variables were used to assess the associations between clinicopathological variables and molecular subtypes, gene expression signatures, baseline serum and tissue protein levels of SDC1 and MMP7. Overall survival (OS) and cancer-specific survival (CSS) were analyzed by Kaplan-Meier log-rank test and Cox regression analysis. In the survival analyses, patient cohorts were stratified by molecular subtypes, gene expression signatures, chemotherapy treatment (chemo vs non-chemo subgroups), the median gene expression of 12 single chemotherapy markers, and levels of serum and tissue SDC1, MMP7, CLDN4 and ERCC1. For multivariate analysis, Cox regression model was used for the parameters with a p-value of <0.05 in the univariate analysis. Gene expression patterns of various molecular subtypes were visualized on heatmaps (Morpheus, https://software.broadinstitute.org/morpheus). All statistical analyses were performed using the SPSS software package (IBM SPSS Statistics for Windows, version 25, IBM Corp., Armonk, NY). All tests with a p value of <0.05 were considered statistically significant.

4. Results

4.1 Development of classifier methods using reduced gene sets

As the first step, we selected markers with the highest discriminative value between molecular subtypes of the TCGA study (29). The marker set was completed with further genes to reach a better discriminating effect also for MDA, LundTax, and Consensus subtypes. Finally, a panel with 68 genes was defined for using molecular subtype classification according to the above-described four classification systems. These genes covered eight signatures; five tumor cell-specific and three stromal signatures. Tumor cell-specific signature scores were: basal/squamous (*CD44, CDH3, COL17A1, KRT14, KRT16, KRT1, KRT5, KRT6A, KRT6B* / *DSC2, DSC3, DSG2, DSG3, GSDMC, PI3, TGM1, TP63*), luminal (*CYP2J2, ERBB2, ERBB3, FGFR3, FOXA1, GATA3, KRT20, PPARG, UPK1A, UPK2*), carcinoma in situ (CIS) (*CRTAC1, CTSE, MSN, NR3C1, PADI3*), neuronal (*CHGA, CHGB, ENO2, GNG4, NCAM1, PEG10, PLEKHG4B, SCG2, SOX2, TUBB2B*), or epithelial-mesenchymal transition (EMT) (*CDH2, SNAI1, TWIST1, VIM, ZEB1, ZEB2*). Stroma-specific signatures were: p53 (*ACTC1, ACTG2, CNN1, DES, FLNC, MFAP4, MYH11, PCP4, PGM5*), extracellular matrix (ECM)/smooth muscle (SM) (*C7, COMP, SFRP4, SGDC*), immune cells (*CD274, CXCL11, IDO1, L1CAM, PDCD1LGZ, SAA1*). The *CDKN2A* gene was added for molecular subtyping of LundTax and Consensus classifications.

As a next step, a classifier method was developed by using publicly available data sets with available transcriptome-based molecular subtype information. Datasets were filtered for the previously selected 68 genes, and all other genes were excluded from the further analyses. For each 68 gene an expression score (ranging from 1 to 5) was calculated based on their relative gene expression in the given patient cohort. Thereby the samples were divided into five groups and received scores (1 – the lowest, 5 – the highest) according to the gene expression levels. Next, an average gene-expression score of the respective genes for the eight signatures (luminal, basal/squamous, neuronal, CIS, EMT, ECM, p53, immune) were calculated. Then, a stepwise classifications system, a so-called "rule set" was established for the TCGA, MDA, LundTax, and Consensus classification systems, respectively. Each rule set was optimized on a training cohort, by adjusting two parameters: 1) cut-offs for signature scores into high and low groups and 2) the sequence of selection steps into different subtypes. These parameters were optimized until the

highest overlap has been reached between the rule set-based and transcriptome-based classifiers. Then, the so optimized rule set-based classifiers were validated on independent public data sets with available transcriptome-based subtype information. Figure 5 summarizes the required steps to develop our classifier method using the reduced gene set.

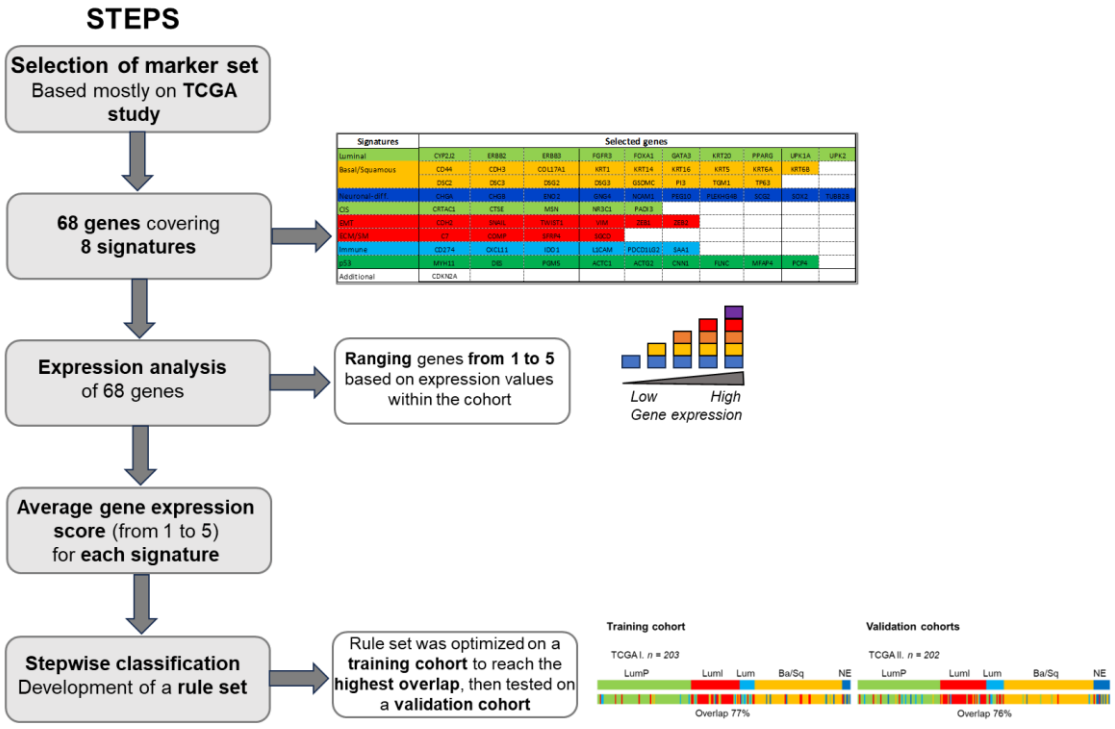

Figure 5. Overview of the steps involved in developing a classification method using reduced gene sets.

For the definition of the TCGA classifier, we randomly divided the TCGA data set (https://tcga-data.nci.nih.gov/tcga/) into a training (n=203) and validation dataset (n=202) (29). For the MDA classifier, we used the GSE48075 data set as the training cohort (n=73) and the TCGA data set as the validation cohort (n=231) (25, 35). For the LundTax classifier, we used the GSE83586 dataset and divided it into a training (n=154) and a validation cohort (n=153) (27). Finally, for the development of Consensus classifier, we divided the TCGA dataset into a training (n=201) and a validation dataset (n=202).

Figure 6 shows the overlaps between the original transcriptome-based classifiers and the rule set-based classifiers. For the TCGA classifier, our method reached a 77%

overlap in the training, and 79% in the validation cohort. The overlap between the rule set-based method for the MDA classification proved to be 81% and 76% in the training and validation cohorts, respectively. The overlap reached 65% and 69% in the Lund training and validation cohorts, while for the Consensus classifier, our method reached 75% and 70% accuracy in the training and validation data sets (Figure 6).

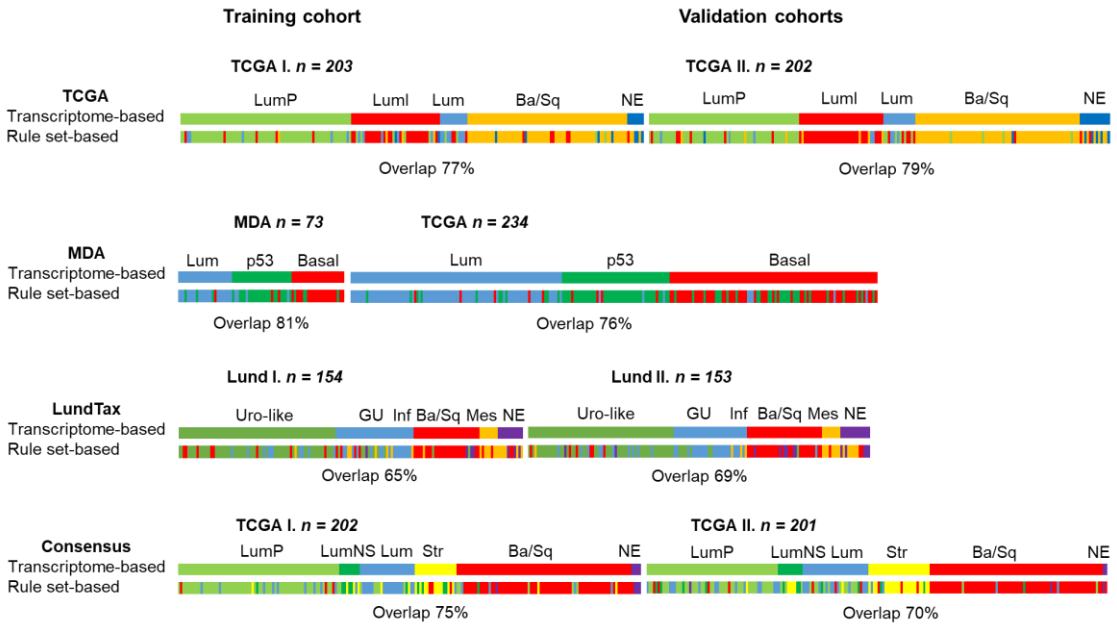

Figure 6. Overlaps between original transcriptome-based classifiers and our newly developed gene and rule set-based classifiers in the training and validation cohorts. Ba/Sq: Basal/Squamous, Ba/SCC-like: Basal/SCC-like, GU: Genomically unstable, Lum: Luminal, LumI: Luminal-infiltrated, LumNS: Luminal non specified, LumP: Luminal-papillary, LumU: Luminal unstable, Mes-like: Mesenchymal-like, Ne: Neuronal, Ne-like: Neuroendocrine-like, Sc/Ne-like: Small-cell/Neuroendocrine-like, Str: Stroma-rich, Uro-like: Urothelial-like.

4.2 Application of the newly developed classifier method to our institutional cohort of 100 RC-treated BC patients

We applied the newly developed subtype classification method to our own institutional cohort of 100 RC frozen MIBC tissue samples. For this, each biopsy was re-evaluated by a board pathologist. Only samples with more than 50% tumor cell content were processed for RNA isolation. After reverse transcription, cDNA samples were used for real-time quantitative PCR with 68 genes by using the TaqMan Array Card technology. The determined relative gene expression values were used for molecular subtype classification according to various systems (MDA, LundTax, TCGA, Consensus) applying our newly elaborated subtype classifier method. Subtype information was than correlated with clinicopathological and follow-up data.

The main characteristics of the institutional cohort (Essen) and the examined publicly available datasets, such as TCGA, MDA, and Lund are summarized in Table 2. In our institutional cohort, the median follow-up time was 10 months with a maximum of 186 months. The clinicopathological data of distinct cohorts are well comparable. However, the presence of pT4 tumors was higher in the Essen cohort, moreover, the survival was shorter in the Essen compared to the TCGA cohort. Molecular subtype distribution was similar between our institutional cohort and those of published reference cohorts (TCGA, MDA, Lund) (Table 2).

Table 2. Patients' characteristics. BC: bladder cancer, LN+: lymph node metastasis, M+: distant metastasis, Gen: genomically, Sc/Ne-like: small-cell/neuroendocrine-like, n.a.: not available data.

Variables		**Essen**	**TCGA**	**MDA**	**Lund**
		n (%)	n (%)	n (%)	n (%)
Age median [range]		65 [36-95]	69 [34-90]	69 [n.a]	70 [38-87]
Sex (male)		69 (69)	304 (74)	54 (74)	240 (78)
Examined BCa samples		100	408	73	307
Stage	≤pT1	0	1 (~0.2)	10 (14)	40 (13)
	pT2	23 (23)	123 (30)	10 (14)	126 (41)
	pT3	45 (45)	196 (48)	25 (34)	86 (28)
	pT4	32 (32)	59 (14)	12 (16)	28 (9)
	pTx	0	33 (8)	16 (22)	6 (2)
	n.a.				21 (7)
Metastases	LN+	35 (35)	132 (32)	23 (32)	14 (~5)
	M+	4 (4)	11 (~3)	n.a	0 (0)
Overall survival (patients alive)					
	1 y	45 (45)	328 (81)	n.a	n.a
	2 y	31 (31)	263 (65)	n.a	n.a
	3 y	27 (27)	246 (60)	n.a	n.a
	4 y	24 (24)	240 (59)	n.a	n.a
	5 y	22 (22)	236 (58)	n.a	n.a
mRNA profiling method		TaqMan Array Card	Illumina HiSeq	Illumina HiSeq	Affymetrix HG 1.0 ST
TCGA	Luminal-papillary	36 (36)	141 (35)	-	-
	Luminal-infiltrated	18 (18)	76 (19)	-	-
	Luminal	4 (4)	26 (6)	-	-
	Basal/Squamous	39 (39)	142 (35)	-	-
	Neuronal	3 (3)	20 (5)	-	-
MDA	Luminal	36 (36)	-	24 (33)	-
	Basal	27 (27)	-	23 (32)	-
	p53-like	37 (37)	-	26 (36)	-
LundTax	Urothelial-like	27 (42)	-	-	133 (43)
	Gen. unstable	7 (11)	-	-	66 (21)
	Infiltrated	-	-	-	6 (2)
	Basal/SCC-like	20 (31)	-	-	62 (20)
	Mesenchymal-like	5 (8)	-	-	16 (5)
	SC/Ne-like	5 (8)	-	-	24 (8)
Consensus	Luminal papillary	17 (27)	127 (32)	-	-
	Luminal non specified	6 (9)	20 (5)	-	-
	Luminal unstable	10 (16)	53 (13)	-	-
	Stroma-rich	1 (~2)	45 (11)	-	-
	Basal/Squamous	29 (45)	152 (38)	-	-
	Neuroendocrine-like	1 (~2)	6 (~1.5)	-	-

Figure 7 represents the overlaps between subtypes determined by our TCGA, MDA, LundTax, and Consensus rule set-based classifiers in our institutional cohort. The *CDKN2A* gene expression was used for LundTax and Consensus classifications and was additionally measured in 64 cases when enough RNA samples remained after the first analysis. Thus, the LundTax and Consensus classifications included only 64 MIBC samples, instead of 100. According to the results of Pearson's Chi^2 test between "summa luminal" (combined: luminal-papillary, luminal-infiltrated, and luminal), basal/squamous subtypes and main clinicopathological parameters, basal/squamous subtype tended to more frequently occur in women *(p=0.069)* then in men. This is in line with the results of the findings of the TCGA study. The subtypes showed no associations with other clinicopathological parameters.

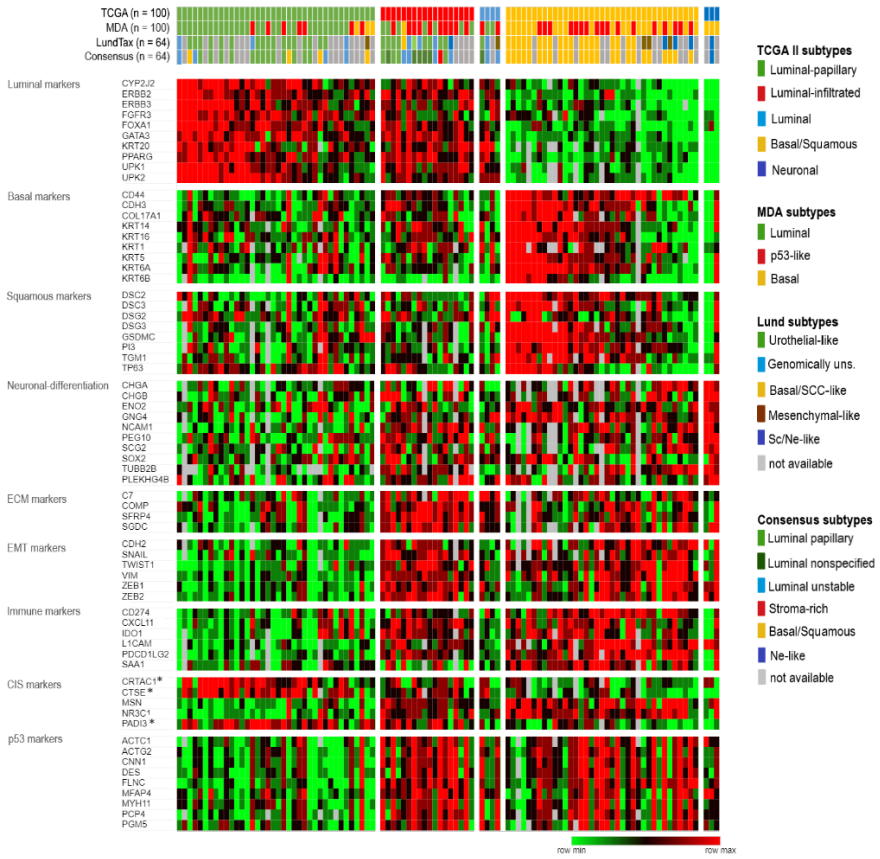

Figure 7. Molecular subtypes determined by rule set-based classifiers and their distinct gene expression profile on our institutional cohort visualized by heatmap. Genes that are downregulated* in CIS. CIS: carcinoma in situ. MDA: MD Anderson, TCGA: The Cancer Genome Atlas. Figure 7 has been published in the article: *Olah C, Hahnen C, Nagy N, et al. A quantitative polymerase chain reaction based method for molecular subtype classification of urinary bladder cancer-Stromal gene expressions show higher prognostic values than intrinsic tumor genes. Int J Cancer. 2022;150(5):856-867. doi:10.1002/ijc.33809*

The luminal-papillary and neuronal subtypes according to TCGA and Consensus classification proved to be prognostic. The TCGA study identified the luminal-papillary tumors to have the longest survival, while those with neuronal tumors had the poorest prognosis. Accordingly, our survival analysis confirmed the poor survival of neuronal tumors, however, could not confirm the favorable prognosis of luminal-papillary tumors (Figure 8).

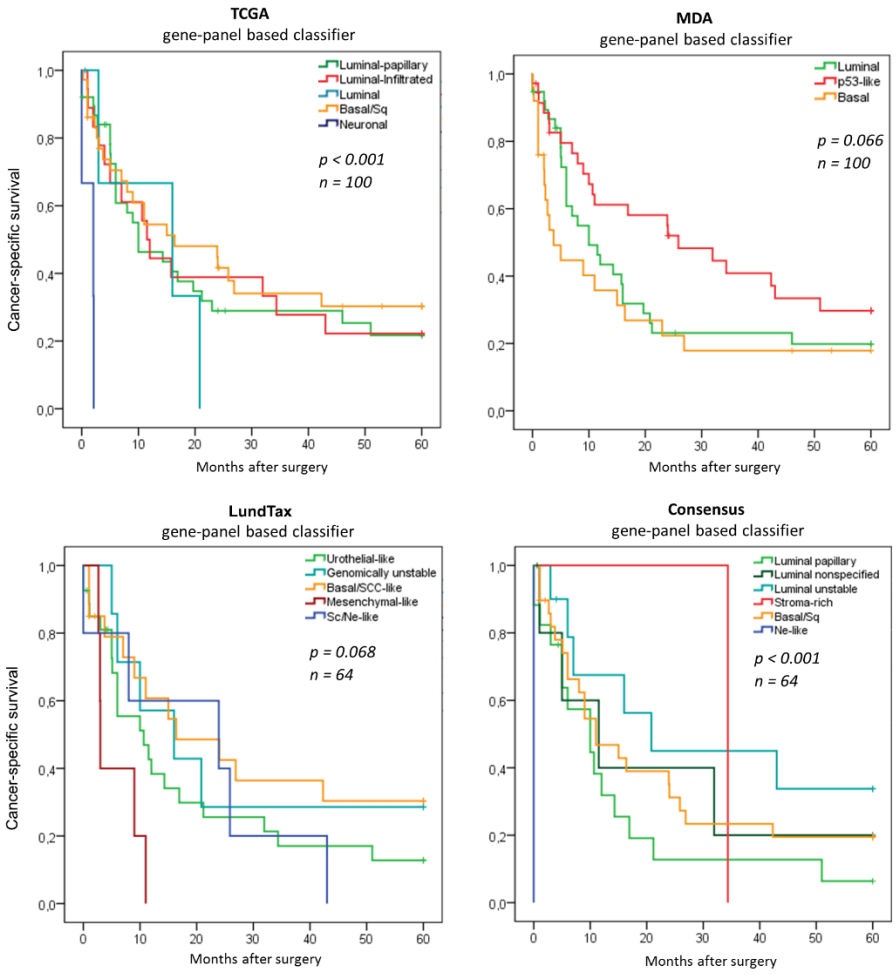

Figure 8. Cancer-specific survival stratified by molecular subtypes according to rule set-based classifiers in our institutional cohort. Basal/Sq: basal/squamous, MDA: MD Anderson, Ne-like: neuroendocrine-like, Sc/Ne-like: small-cell/neuroendocrine-like, TCGA: The Cancer Genome Atlas. Figure 8 has been published in the article*: Olah C, Hahnen C, Nagy N, et al. A quantitative polymerase chain reaction based method for molecular subtype classification of urinary bladder cancer-Stromal gene expressions show higher prognostic values than intrinsic tumor genes. Int J Cancer. 2022;150(5):856-867. doi:10.1002/ijc.33809*

In addition to the clinicopathological parameters, the prognostic values of the signature scores were evaluated by Cox univariate analysis. Multivariate analyses included those variables with a p-value of <0.05 in the univariate analyses (Table 3A and

B). The presence of lymph node metastasis was associated with worse overall (OS) and cancer-specific survival (CSS) *(p<0.001)*, while higher pT-stage was associated with poor CSS *(p=0.014)*. Basal, squamous, luminal, EMT, and CIS signature scores had no impact on survival. On the other hand, the high neuronal signature was a risk factor for OS and CSS *(p<0.001)*, while high ECM, immune, and p53 signatures were associated with longer OS *(p=0.001, p=0.001, p=0.023)* and CSS *(p=0.002, p=0.006, p=0.004)* (Table 3A). The multivariate analysis confirmed the presence of lymph node metastases and high neuronal signature score as independent risk factors for OS and CSS, *(p<0.001 and p<0.001)*. In addition, the high immune score was independently associated with prolonged OS *(p=0.039)*, and high ECM score with better CSS *(p=0.049)* (Table 3B).

Table 3. Cox uni- and multivariate survival analyses with dichotomized signature scores on our institutional cohort.

A Univariate analysis	**Overall survival**			**Cancer-specific survival**		
		n=100			n=100	
Variables	HR	95% CI	P	HR	95% CI	P
Age (>65)	1.064	0.671-1.687	0.792	0.978	0.597-1.602	0.929
Sex (female)	1.548	0.915-2.620	0.103	1.498	0.848-2.647	0.164
Stage (>pT3)	1.137	0.974-1.328	0.104	1.835	1.131-2.977	**0.014**
Metastases						
Lymph node (LN+)	2.429	1.516-3.892	**<0.001**	3.004	1.823-4.950	**<0.001**
Distant (M+)	1.645	0.567-4.766	0.359	1.881	0.641-5.520	0.250
Signature scores						
Basal score (≥3)	0.893	0.571-1.399	0.622	0.761	0.472-1.227	0.262
Squamous score (≥3)	1.059	0.679-1.652	0.800	0.980	0.610-1.573	0.993
Basal/squamous score (≥3)	1.002	0.771-1.302	0.989	0.881	0.548-1.416	0.602
Luminal score (≥3)	1.014	0.652-1.578	0.949	1.053	0.655-1.694	0.830
Neuronal score (≥4.2)	9.714	3.221-29.291	**<0.001**	14.160	4.758-41.822	**<0.001**
EMT score (≥3)	0.705	0.452-1.099	0.123	0.705	0.438-1.134	0.149
ECM score (≥3)	0.450	0.283-0.714	**0.001**	0.468	0.289-0.759	**0.002**
Immune score (≥3)	0.468	0.296-0.738	**0.001**	0.510	0.315-0.826	**0.006**
CIS score (≥3)	0.841	0.540-1.310	0.444	0.811	0.503-1.309	0.392
p53 score (≥3)	0.592	0.376-0.931	**0.023**	0.489	0.300-0.798	**0.004**
B Multivariate analysis						
Variables	HR	95% CI	P	HR	95% CI	P
Stage (>pT3)	-	-	-	1.193	0.718-1.983	0.496
Lymph node (N+)	2.484	1.528-4.039	**<0.001**	3.178	1.863-5.241	**<0.001**
Neuronal score (≥4.2)	12.091	3.602-40.582	**<0.001**	16.376	4.852-55.276	**<0.001**
ECM score (≥3)	0.607	0.362-1.019	0.059	0.551	0.305-0.997	**0.049**
Immune score (≥3)	0.569	0.334-0.971	**0.039**	0.687	0.391-1.206	0.191
p53 score (≥3)	0.886	0.506-1.552	0.673	0.739	0.399-1.369	0.336

4.3 Development of a further reduced marker set for FFPE samples

Based on our experiences collected during the measurements detailed in 4.2 section, we further optimized the marker set. This improvement allowed us to reduce the marker set from 68 to 48 genes. Some genes were excluded, and in addition, some neuronal genes with lower specificity were removed and substituted with other neuronal genes based on literature data (36, 37). The tumor intrinsic signatures included the following genes: basal/squamous (*CD44*, *CDH3*, *KRT14*, *KRT5*, *KRT6A* / *DSC2*, *DSG3*, *PI3*), luminal (*CYP2J2*, *ERBB2*, *FGFR3*, *FOXA1*, *GATA3*, *KRT20*, *PPARG*, *UPK1A*, *UPK2*), carcinoma in situ (*CRTAC1*, *CTSE*, *MSN*, *NR3C1*), neuronal (*APLP1*, *CHGB*, *ENO2*, *GNG4*, *MSI1*, *PEG10*, *PLEKHG4B*, *RND2*, *SV2A*, *TUBB2B*), and epithelial-mesenchymal transition (EMT) (*CDH2*, *TWIST1*, *VIM*, *ZEB1*), while the tumor extrinsic signatures the following genes: p53 (*ACTC1*, *ACTG2*, *CNN1*, *MYH11*, *PGM5*), extracellular matrix (ECM)/smooth muscle (SM) (*COMP*, *SFRP4*, *SGDC*), and immune (*CD274*, *CXCL11*, *IDO1*, *SAA1*). The *CDKN2A* gene was still included in the reduced marker set. The change in the gene set required the adjustment the corresponding classifier rule sets, which resulted in a slight improvement of methodological accuracy (Figure 9).

The above detailed 48-gene set was applied to the NanoString nCounter method. We decided to use this analytical platform, as it is also applicable to low amount and quality RNA samples, which is frequently true for samples isolated from FFPE tumor material. Figure 9 summarizes the overlaps between the original transcriptome-based and rule set-based classifiers with 68 and 48 genes. The TCGA, MDA, and Consensus classifiers with 48 genes reached similar overlaps with the original transcriptome-based classifiers like the rule set with 68 genes (- 1-2%). The LundTax classifier reached higher overlap by the 48-gene marker set (+ 6%) (Figure 9).

As a final step, we determined the expression values of the 48 genes in our institutional cohort with FFPE MIBC samples by the NanoString nCounter technique and identified the molecular subtypes by the rule set-based classifiers. In the following sections, the molecular subtyping was performed using the 48-gene marker set.

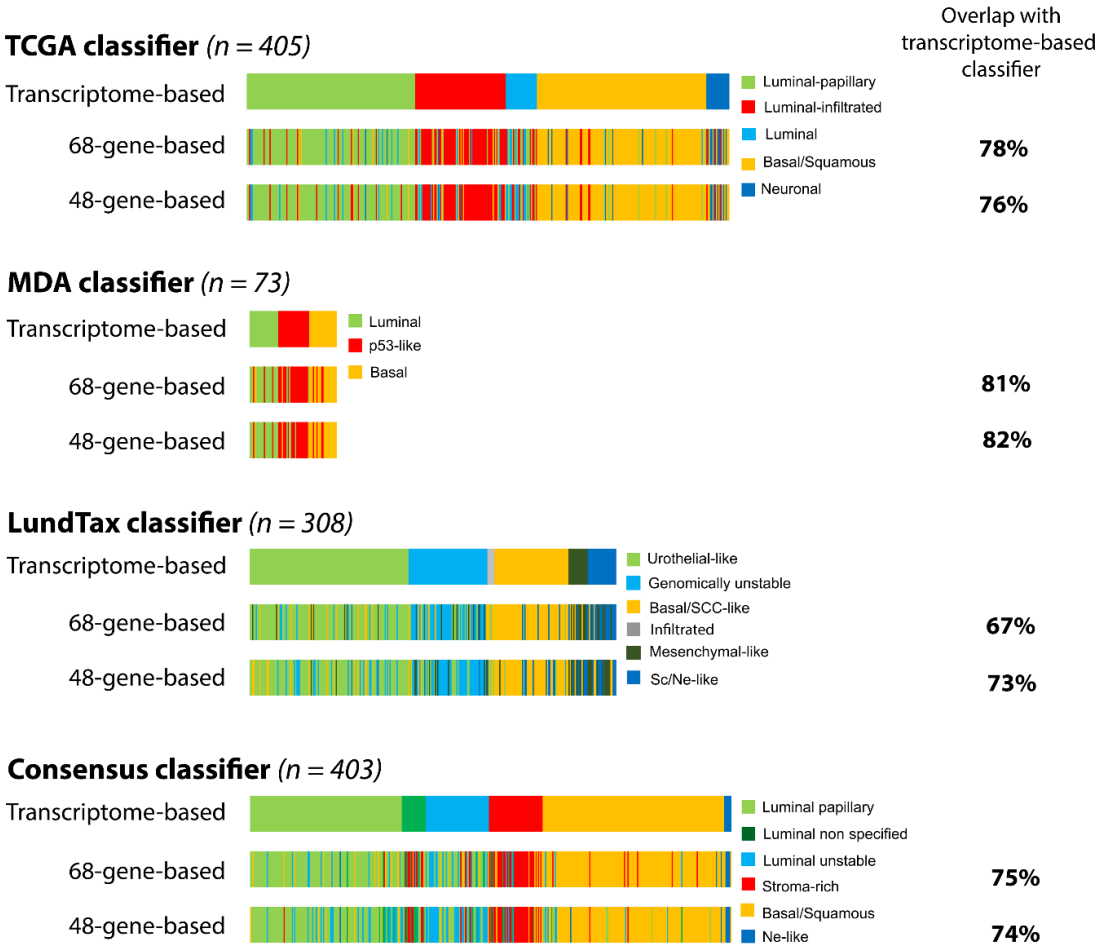

Figure 9. Overlaps between original transcriptome-based and rule set-based classifiers with 68-gene and 48-gene marker sets for fresh frozen and FFPE samples. MDA: MD Anderson, Ne-like: neuroendocrine-like, Sc/Ne-like: small-cell/neuroendocrine-like, TCGA: The Cancer Genome Atlas. Figure 9 has been partly published in the article*: Olah C, Szarvas T. A Panel-Based Method for the Reproduction of Distinct Molecular Subtype Classifications of Muscle-Invasive Urothelial Bladder Cancer. Methods Mol Biol. 2023;2684:27-43. doi:10.1007/978-1-0716-3291-8_2*

4.4 Application of the above developed classifier methods to our own institutional cohort of patients with pT3/4 or LN-positive BC, who did or did not receive adjuvant chemotherapy

Our study included 160 MIBC patients who underwent RC and had a pT3/4 or LN positive histological finding, which represents an indication for adjuvant chemotherapy. None of the patients received NAC before RC. Approximately the half of these patients received adjuvant platinum-based chemotherapy (chemo cohort, n=81), while the other half of the patients refused or were ineligible to chemotherapy (non-chemo cohort, n=79). The chemo and non-chemo cohorts were comparable in terms of male/female ratio, stage at RC, the presence of lymphovascular and vascular invasion, and surgical margin. On

the other hand, the occurrence of LN positivity was higher in the chemo cohort, whil the median age in the non-chemo cohort (*p=0.007*, *p=0.008*, respectively, according to Chi^2 test and Mann-Whitney tests). The median OS tended to be longer for chemo patients compared to non-chemo patients (18.2 vs 8.2 months, *p=0.069*). The distribution of distinct molecular subtypes was similar according to each classifier system between the chemo and non-chemo cohorts (Table 4).

We performed a Chi^2 test to assess correlations between clinicopathological variables and molecular subtypes. The luminal-papillary subtype (according to TCGA and Consensus classifications), the luminal (according to MDA), and the urothelial-like (according to LundTax) were used as reference groups. The basal subtypes (according to the TCGA, LundTax, and Consensus classifications) occurred more frequently in women (*p=0.018*, *p=0.021*, and *p=0.050*, respectively). On the other hand, lymphovascular invasion was less frequent in basal and neuronal (Ne) subtypes (TCGA: *p=0.018* and *p=0.008*, MDA: *p=0.006*, LundTax: *p=0.005* and *p=0.018*, Consensus: *p=0.066* and *p=0.020*). The occurrence of vascular invasion was significantly higher in the mesenchymal-like subtype (LundTax: *p=0.014*). The presence of LN+ was significantly less frequent in basal tumors according to each classifier (TCGA: *p=0.020*, MDA: *p=0.008*, LundTax: *p=0.002*, Consensus: *p=0.010*).

Table 4. Patients' characteristics of the MIBC FFPE cohort (n=160). Ba/Sq: Basal/Squamous, Ba/SCC-like: Basal/SCC-like, GU: Genomically unstable, Lum: Luminal, LumI: Luminal-infiltrated, LumNS: Luminal non specified, LumP: Luminal-papillary, LumU: Luminal unstable, Mes-like: Mesenchymal-like, n.a.: not available, Ne: Neuronal, Ne-like: Neuroendocrine-like, RC: radical cystectomy, Sc/Ne-like: Small-cell/Neuroendocrine-like, Uro-like: Urothelial-like.

variables		**Non-chemo cohort** n (%)	**Chemo cohort** n (%)
Total number of patients		79	81
Age at baseline median [range]		72 [48-90]	63 [39-82]
Sex	male	60 (76)	53 (65)
	female	19 (24)	28 (35)
Cystectomy data	pT1	-	1 (1)
	pT2	4 (5)	15 (19)
	pT3	55 (70)	39 (48)
	pT4	20 (25)	21 (26)
	n.a.	0	5 (5)
Lymphovascular invasion	L0	36 (46)	39 (48)
	L+	43 (54)	39 (48)
	n.a.	0	3 (4)
Vascular invasion	V0	63 (80)	56 (69)
	V+	16 (20)	24 (30)
	n.a.	0	1 (1)
Surgical margin	R-	60 (76)	41 (50)
	R+	18 (23)	16 (20)
	n.a.	1 (1)	24 (30)
Lymph node metastasis at RC	LN0	50 (63)	34 (42)
	LN+	29 (37)	47 (58)
Number of patients died (%)		62 (78)	54 (67)
Follow-up time in months median (range)		8.2 (0-163)	18.2 (1-157)
Subtype class information			
TCGA	LumP	16 (20)	21 (26)
	LumI	12 (15)	15 (18)
	Lum	14 (18)	13 (16)
	Ba/Sq	33 (32)	29 (36)
	Ne	4 (5)	3 (4)
MDA	Luminal	13 (16)	23 (28)
	Basal	28 (35)	28 (34)
	p53-like	38 (48)	30 (37)
LundTax	Uro-like	27 (34)	33 (41)
	GU	14 (18)	13 (16)
	Ba/SCC-like	24 (30)	23 (28)
	Mes-like	10 (13)	9 (11)
	Sc/Ne-like	4 (5)	3 (4)
Consensus	LumP	21 (27)	26 (32)
	LumNS	1 (1)	4 (5)
	LumU	7 (9)	7 (9)
	Stroma-rich	8 (10)	6 (7)
	Ba/Sq	38 (48)	35 (43)
	Ne-like	4 (5)	3 (4)

Samples were classified into molecular subtypes according to different classification systems (TCGA, LundTax, MDA, Consensus) by using our gene panel and classifier method (see section 4.3). OS analyses were performed by the Kaplan-Meier method (and long rank test) by plotting chemo-treated and untreated patients within each molecular subtype. Based on this approach, tumors with luminal-papillary subtypes (according to TCGA and Consensus classifications; $p=0.036$ and $p=0.009$, respectively) and urothelial-like subtype (according to LundTax; $p=0.001$) classification proved to benefit from adjuvant chemotherapy by significant longer OS. On the contrary, the tumors with basal subtypes showed similar survival rates in the chemo and non-chemo groups (Figure 10), suggesting that tumors with basal molecular subtype are not sensitive to adjuvant platinum therapy.

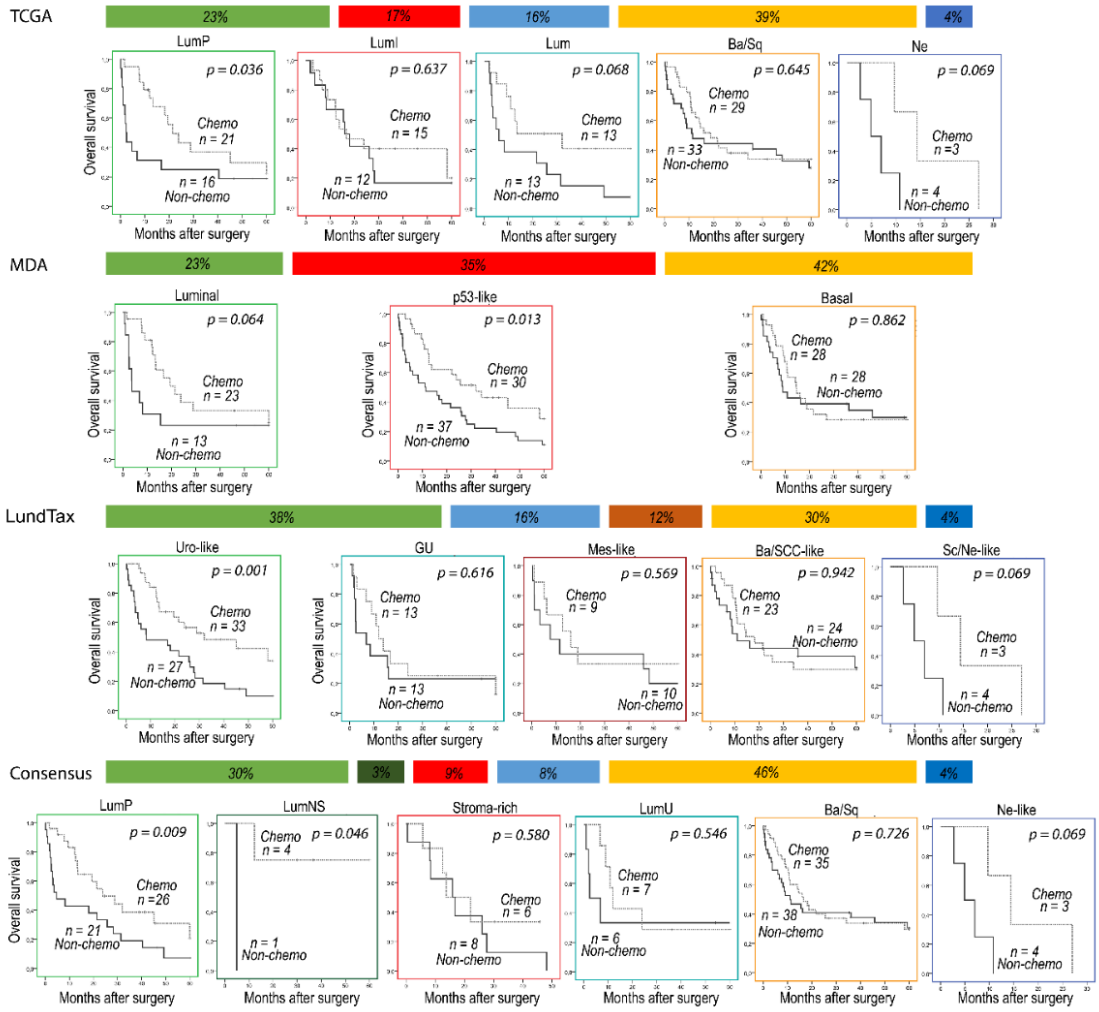

Figure 10. Survival analysis curves stratified by chemotherapy (chemo vs non-chemo). The molecular subtypes were identified with rule set-based classifiers. Ba/Sq: Basal/Squamous, Ba/SCC-like: Basal/SCC-like, GU: Genomically unstable, Lum: Luminal, LumI: Luminal-infiltrated, LumNS: Luminal non specified, LumP: Luminal-papillary, LumU: Luminal unstable, Mes-like: Mesenchymal-like, Ne: Neuronal, Ne-like: Neuroendocrine-like, Sc/Ne-like: Small-cell/Neuroendocrine-like, Uro-like: Urothelial-like. Figure 10 has been published in the article: *Olah C, Reis H, Hoffmann MJ, et al. Predictive value of molecular subtypes and APOBEC3G for adjuvant chemotherapy in urothelial bladder cancer. Cancer Med. 2023;12(5):5222-5232. doi:10.1002/cam4.5324*

4.5 Single genes for chemotherapy prediction

4.5.1 Discovery analysis on our institutional patient cohorts

In addition to the 48 subtype-specific genes (see section 4.3), we selected 12 additional potentially platinum-predictive genes for NanoString gene expression analysis. These genes were selected based on own, yet unpublished research (*APOBEC3A, APOBEC3B, APOBEC3G, TOP2A, BSG, MMP7*) as well as on literature data (*BIRC5, CDK12, CLDN4, ERCC1, HMGA2* and *MKI67)*.

The continuous gene expression values were correlated with clinicopathological variables using the Mann-Whitney test. *APOBEC3G* and *MMP7* gene expressions were higher in women (*p=0.017* and *p=0.044*, respectively). Lower *MMP7* expression correlated with lymphovascular invasion *(p=0.008)*, while lower gene expression values of *APOBEC3G* and *MKI67* showed a correlation with surgical margin positivity (*p=0.010* and *p=0.018*, respectively).

For correlation analyses, the median gene expression values were used as a cut-off to divide patients into marker-high and marker-low expression groups. The same approach was applied for the evaluation of 12 individual genes as in the case of molecular subtypes (section 4.4); the OS rate was directly compared between chemotherapy-treated and untreated patient cohorts within marker low and high subgroups (Figure 11). The markers can be divided into three groups:

1) favorable factors with improved outcome in the chemotherapy cohort (*APOBEC3G; p=0.002, CLDN4; p=0.004, ERCC1; p=0.003*) (Figure 11A),
2) risk factors with poor survival in the chemotherapy cohort (*BIRC5; p=0.007, HMGA2; p=0.005, MKI67; p=0.002*) (Figure 11B),
3) factors with no association with the outcome (*APOBEC3A, APOBEC3B, CDK12, BSG, MMP7, TOP2A*) (Figure 11C).

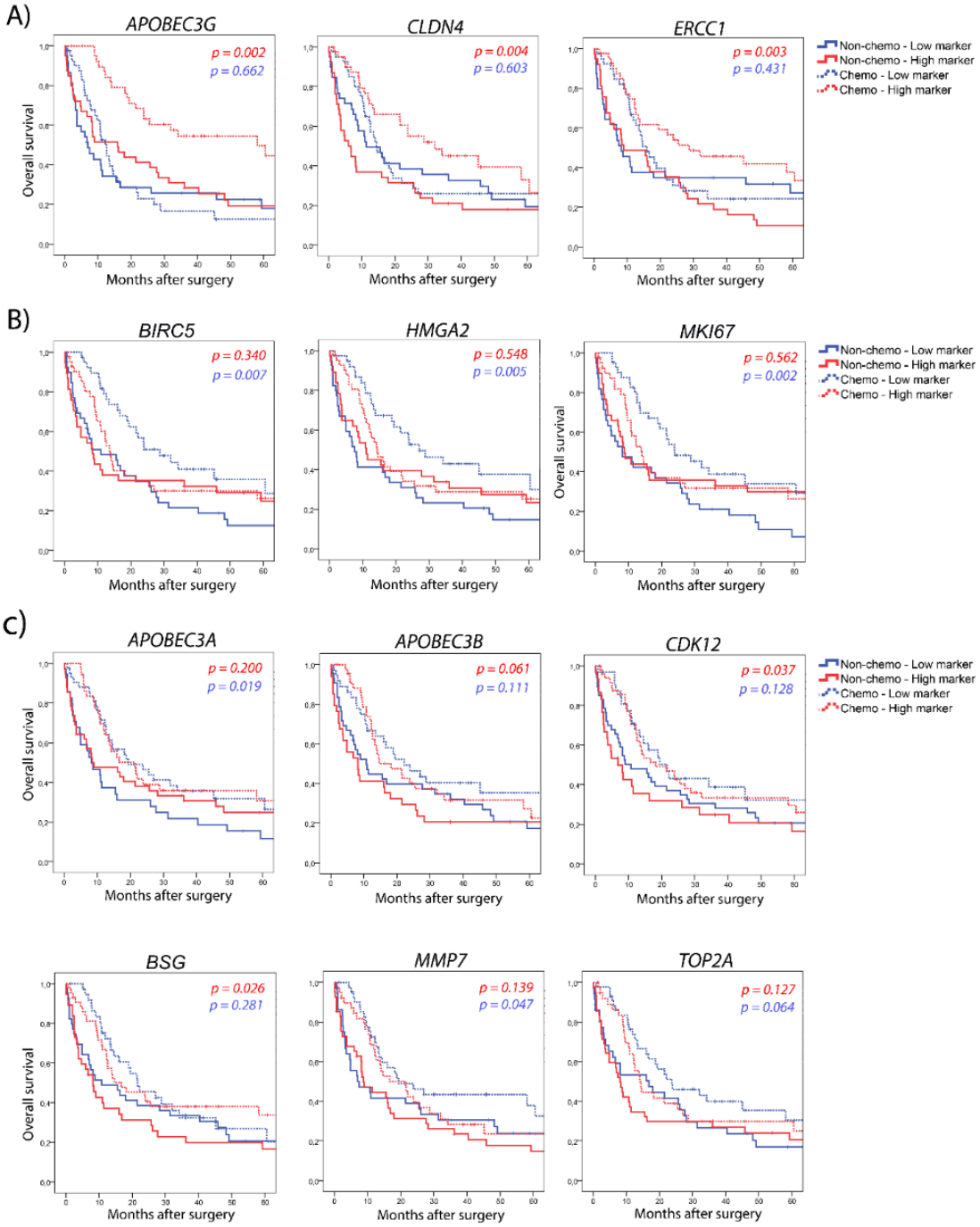

Figure 11. Overall survival stratified by low and high gene expression values and chemotherapy treatments (chemo *vs.* non-chemo) in our institutional cohort (n=160). P-values represent OS difference between platinum-treated and untreated patients in the high (red) and low expression (blue) biomarker groups. Predictive (A) and risk (B) genes in chemotherapy-treated patients are grouped separately from markers not associated with patients' survival outcome (C). Figure 11 has been published in the article: *Olah C, Reis H, Hoffmann MJ, et al. Predictive value of molecular subtypes and APOBEC3G for adjuvant chemotherapy in urothelial bladder cancer. Cancer Med. 2023;12(5):5222-5232. doi:10.1002/cam4.5324*

4.5.2 Validation analysis in a published NAC dataset

Next, we aimed to validate the chemotherapy predictive values of the above identified six genes (see section 4.5.1) on an independent publicly available transcriptome dataset from patients who received NAC (n=125) or upfront RC without chemotherapy (n=161) (Lund cohorts) (28). The high gene expression value of *APOBEC3G* and *CLDN4* identified patients with improved OS in the NAC (*p=0.026* and *p=0.025*, respectively), but not in the upfront RC cohort (*p=0.576* and *p=0.493*, respectively), which confirmed the chemotherapy predictive value of these two genes (Figures 12A and C). In addition, the low gene expression value of *BIRC5* also identified patients with favorable OS after chemotherapy-treatment *(p=0.032)* (Figure 12E). For the NAC cohort the pathological complete response (pCR) rates were also available. By assessing this endpoint only *APOBEC3G* showed a significant association, as its higher levels were significantly correlated with higher pCR rates *(p=0.028)* (Figure 12B, D and F). High *ERCC1* gene expression and low gene expressions of *HMGA2* and *MKI67* were associated with improved OS in our institutional cohort. However, in the validation (Lund) cohort, the opposite result was observed, as patients with low *ERCC1* gene expressions tended to benefit from chemotherapy *(p=0.052)*. The high gene expression values of *HMGA2* and *MKI67* tended to be associated with worse survival rates in the chemotherapy-treated cohort, but these associations did not reach the significance level (*p=0.059* and *p=0.345*, respectively).

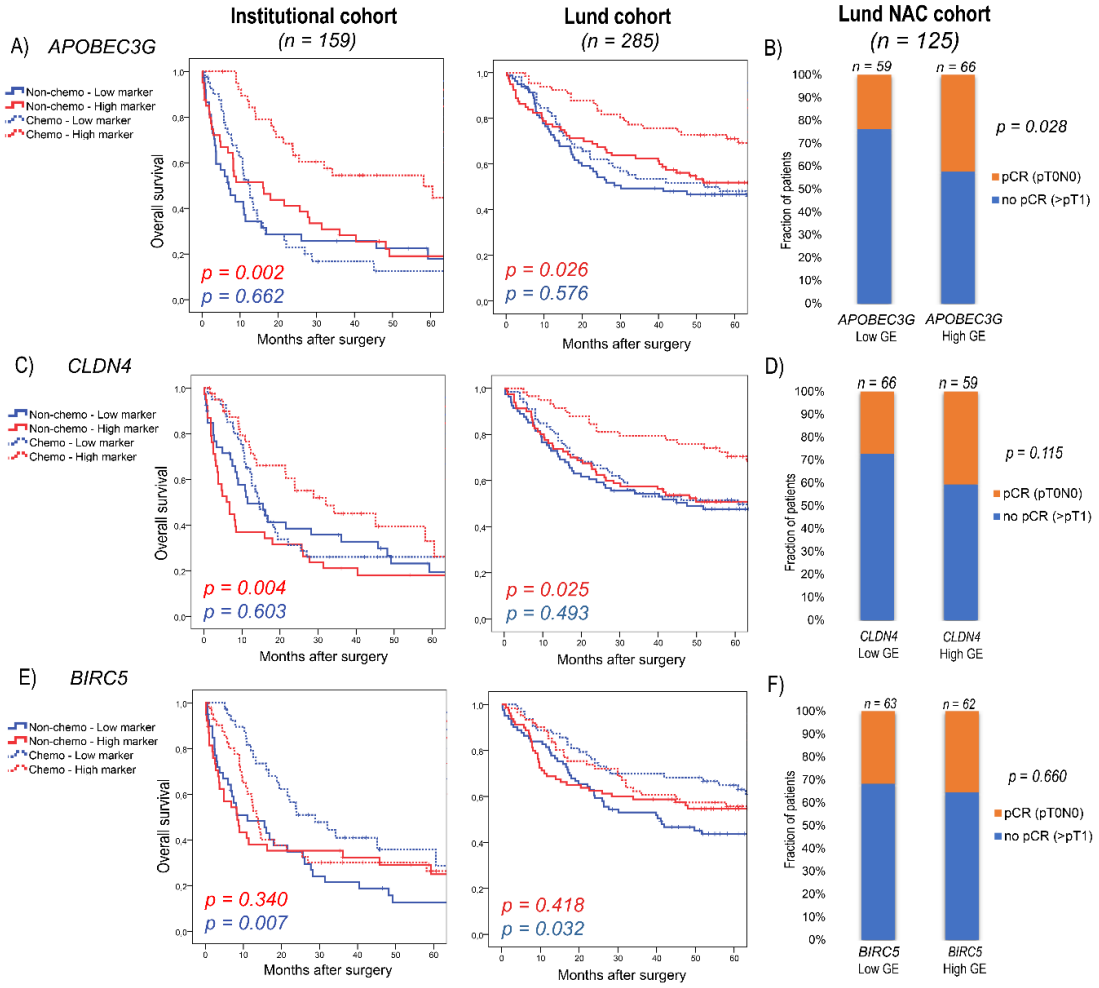

Figure 12. Overall survival stratified by low and high gene expressions in our institutional (n=159) and validation (Lund) (n=285) cohorts (A, C, E). Pathological response rates for NAC in low and high gene expression groups in the validation (Lund) cohort (B, D, F). P-values represent OS difference between platinum-treated and untreated patients in the subgroups with high gene expression (red) and low gene expression (blue) levels. Figure 12 has been published in the article: *Olah C, Reis H, Hoffmann MJ, et al. Predictive value of molecular subtypes and APOBEC3G for adjuvant chemotherapy in urothelial bladder cancer. Cancer Med. 2023;12(5):5222-5232. doi:10.1002/cam4.5324*

4.5.3 Protein expression of CLDN4 and ERCC1

In a former analysis (unpublished results), the protein expression of CLDN4 and ERCC1 were investigated by IHC in our institutional MIBC cohort with patients who received postoperative chemotherapy. The examined cohort are partly overlapping with the IHC cohort presented in the 4.6 section. The results of CLDN4 were in accordance with the gene expression results, as the high CLDN4 expression was associated with improved OS after the chemotherapy *(p=0.017)* (Figure 13A). However, the results of ERCC1 protein expression were contrary to our current gene expression results as high ERCC1 protein expression tended to associate with shorter OS *(p=0.061)*, thus showing similarity to the results found in the validation (Lund) dataset at gene expression level (Figure 13B).

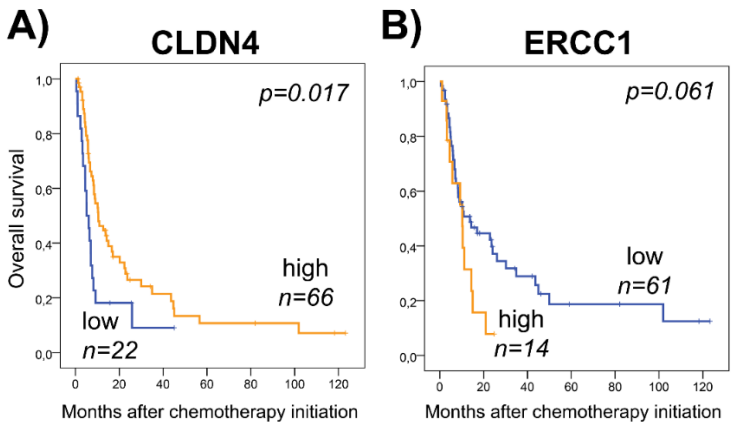

Figure 13. Overall survival stratified by protein expressions of CLDN4 (A) and ERCC1 (B) in MIBC patients treated with postoperative chemotherapy.

4.6 Serum markers for chemotherapy prediction

The analysis of chemotherapy-predictive proteins secreted in the blood may be easily applied into the daily clinical routine. Therefore, we aimed to examine the baseline serum levels of SDC1 and MMP7 in the institutional chemotherapy-treated MIBC cohort. SDC1 and MMP7 were shown to be involved in chemotherapy resistance (38, 39), moreover MMP7 - a member of matrix-metalloproteinase family - is involved in the proteolytic ectodomain shedding of several transmembrane proteins including SDC1 (40). Therefore, we aimed to assess the potential platinum-predictive value of MMP7 and SDC1 in urothelial BC.

Our institutional cohort included 52 MIBC patients, who received postoperative platinum therapy. Serum samples were collected directly before the first chemotherapy treatment and were stored at -80°C until ELISA analysis. In addition, SDC1 and MMP7 protein expressions were assessed by IHC in FFPE tissue samples of patients who underwent later postoperative chemotherapy (n=72). Of note, there was no overlap between the patient cohorts with available serum and tissue cohorts, therefore a direct comparison between tissue IHC and serum ELISA results was not possible. Table 5 summarize patients' characteristics of the "serum" and "IHC" cohorts.

Table 5. Patients' characteristics in serum and IHC cohorts (no overlap between the two cohorts).

Cohort	**Serum**	**IHC**
Variables	n (%)	n (%)
Total number of patients	52 (100)	72 (100)
Age at baseline median [range]	65 [41-81]	64 [37-90]
≤ 65	27 (52)	37 (51)
> 65	25 (48)	35 (49)
Sex		
male	38 (73)	50 (69)
female	14 (27)	22 (31)
Cystectomy data		
pT1	1 (2)	1 (1)
pT2	9 (17)	16 (22)
pT3	21 (40)	24 (33)
pT4	10 (20)	13 (18)
n.a.	11 (21)	18 (25)
Metastases		
Lymph node metastasis (>2cm)	34 (65)	31 (43)
Distant metastasis	12 (23)	19 (26)
Soft tissue lesions (lung/liver)	9 (17)	28 (39)
Bone metastasis	3 (6)	9 (13)
Number of patients died	31 (60)	53 (74)
Follow-up time in months median [range]	16 [2-101]	9 [1-102]

The cut-off of serum SDC1 for dichotomization was determined as the upper 25th percentile (180 ng/mL), while the cut-off of serum MMP7 was determined at the median. High serum SDC1 and MMP7 levels were associated with shorter OS (*p=0.004* and *p=0.033*, respectively) (Figures 14A and B). Membranous, cytoplasmic, and stromal SDC1 protein expressions were separately evaluated. We found no association between

SDC1 tissue expressions and survival outcomes (membranous SDC1: *p=0.918*, cytoplasmic SDC1: *p=0.802*, stromal SDC1: *p=0.452*). MMP7 staining was localized in the cytoplasm of tumor cells, and frequently showed higher expressions at the tumor-stroma interface. High MMP7 tissue expression and serum concentration levels were associated with shorter OS (*p=0.033* and *p=0.017*, respectively) (Figures 14B and C). In addition, we compared serum baseline levels of SDC1 and MMP7 and found higher SDC1 serum levels to be positively correlated with MMP7 serum concentrations (Spearman's rho test; correlation coefficient: 0.326, *p=0.029*) (Figure 14D).

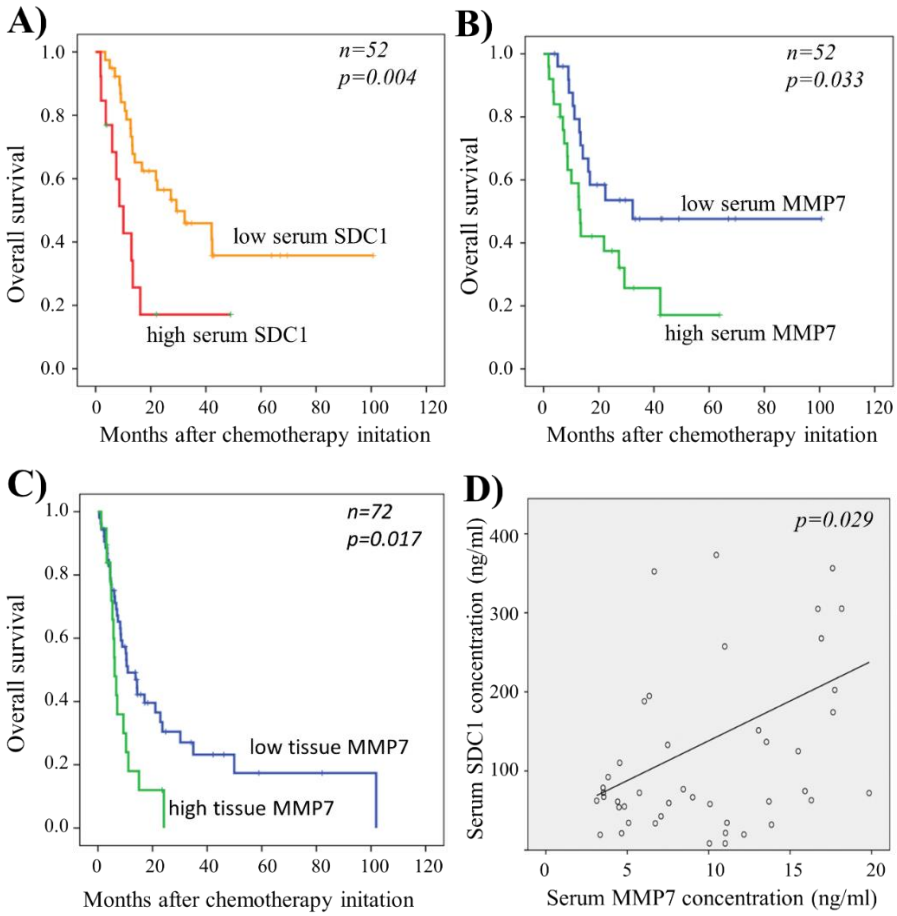

Figure 14. Overall survival stratified by serum SDC1 level (A), serum and tissue MMP7 levels (B and C). Correlations between serum MMP7 and SDC1 levels (D).

5. Discussion

In the present work, we aimed to identify platinum-predictive tissue and serum markers for MIBC patients. Therefore, we developed a simple, robust, and cost-effective gene expression-based classifier method for molecular subtyping, which has been applied to our own institutional cohorts of frozen (n=100) and FFPE samples (n=160), by using the RT-qPCR and NanoString analytical platforms. In addition, based on preliminary results and literature data, we selected and tested 12 single genes and two serum markers, with potential platinum predictive value.

Recently, transcriptome sequencing in various MIBC cohorts has revealed a molecular diversity of urothelial tumors and defined gene expression-based molecular subtypes with distinct clinical behaviors in terms of prognosis and therapy sensitivity. Due to the methodological complexity and high costs of this method, the use of molecular subtypes as prognostic and/or predictive factors could not spread into the clinical routine. However, recently new therapeutic agents have become available after a chemotherapy failure. Therefore, predicting patients' platinum resistance may help to avoid unnecessary exposure to cytotoxic platinum treatments and thus may help to reduce the use of ineffective treatments leading to better patients' prognosis.

Several studies aimed to simplify the molecular subtyping by using gene panel- or IHC-based classifiers. However, these classifiers were only able to differentiate between the luminal and basal subtypes, mostly without correlation analysis to mRNA-based subtypes.

Rinaldetti *et al.* created a 36-gene panel that included luminal, basal, and p53-like gene signatures and classified basal, luminal, and "infiltrated" subtypes. Based on their results, luminal tumors had significantly worse CSS and OS in a MIBC cohort after RC (n=47) (41). A study by Kardos *et al.* developed a NanoString-based method using a 47-gene set. Their panel was able to distinguish between the luminal and basal subtypes, but the so identified subtypes were not associated with patients' prognosis (42). A further study with a reduced gene set, stratified 39 RC treated MIBC patients into luminal, luminal-like, basal, and basal-like subtypes, which are however not compatible with classes according to the original transcriptome-based classification systems. In addition, authors did not find a prognostic value for their subtypes (43).

IHC-based studies typically apply 2-5 proteins for the identification of molecular subtypes. A study by Font *et al.* evaluated the expression of two luminal markers (FOXA1, GATA3) and two basal markers (KRT5/6, and KRT14) in 126 MIBC samples and classified them into luminal-like, basal/squamous-like, and mixed subgroups. They found significantly higher pathological response rate to NAC for basal/squamous-like tumors (31). A further IHC study stratified 106 MIBC tumors into luminal and basal subtypes based on the expressions of GATA3, UPK2, KRT20, KRT5/6, and KRT14 proteins. The basal molecular subtype showed high overlap with the presence of squamous secondary variant histology, while the luminal molecular subtype was associated with pure urothelial carcinoma histology. Moreover, each tumor with micropapillary variant histology was classified into luminal molecular subtype, confirming the accuracy of molecular classification on the histological level. Of note, authors found no differences in patients' survival between luminal and basal molecular subtypes (32). In addition, authors found tumor-associated immune cell status to have a major impact on CSS, as luminal and basal tumors with low immune cell infiltration had significantly worse survival compared luminal and basal tumors with high immune cell infiltration. Thus, this study by Ikeda *et al.* suggest that the tumor microenvironment also plays an important role for the survival, therefore it is necessary to distinguish additional subgroups within the luminal and basal subtypes based on microenvironmental factors (32). The LundTax IHC classifier is different from the above-described IHC-based methods as this aims to identify the same subtypes that were classified by transcriptome-based classifier at the RNA level. In contrast to other classification systems, LundTax aimed to exclude the impact of stromal- and immune cells from the analysis and focused only on the expression patterns of the cancer cells. This method differentiates five subtypes; urothelial-like, genomically unstable, basal/SCC-like, mesenchymal-like, and Sc/Neuroendocrine-like, according to the LundTax mRNA-based classification system. The IHC-based molecular classifier is well-elaborated and described, applying a minimum of 13 protein markers, which makes this method hardly compatible with current pathological practice (27, 44). Overall, other current molecular subtype classifiers with reduced gene sets or protein markers are not able to reproduce the transcriptome-based classifications. They use a heterogeneous set of gene or protein markers, and the identified subtypes are mostly not compared to transcriptome-based subtypes of the same samples.

Therefore, the accuracy of these simplified classification methods cannot be critically evaluated. Therefore, the results on the prognostic and predictive values of different subtypes by these methods are heterogeneous and not comparable to each other.

Our 68-gene panel-based method is the first classifier method with a reduced gene set that can fully reproduce the most widely used transcriptome-based classification systems such as the MDA, TCGA, LundTax, and Consensus. However, our marker set was primarily selected to recapitulate the TCGA classification, we also achieved relatively high overlaps between our 68-gene panel-based classification method and other transcriptome-based classifiers. Our method reached 78%, 81%, 67%, and 75% overlaps for TCGA, MDA, LundTax, and Consensus classifications systems, respectively. After the *in silico* development and validation, we applied our panel- and rule-set-based classification method to our institutional cohort of 100 fresh-frozen MIBC samples. For this, mRNA expression of 68 genes were determined by using the RT-qPCR method, then, samples were classified into distinct molecular subtypes. As a next step, we evaluated the prognostic values of TCGA, MDA, LundTax, and Consensus subtype classifications in our institutional cohort and found that TCGA-neuronal and luminal tumors have the worse survival, which is in line with the findings of the original (TCGA) study (29). Neuronal subtype represents only ~5% of MIBCs but has a devastating prognosis and poor response to NAC. On the other hand, patients with neuronal or luminal subtypes according to the TCGA classifier may benefit from immunotherapy, which makes the distinction of these subtype clinically relevant (29, 36, 45). The TCGA study reported favorable prognosis for luminal-papillary tumors, which was later confirmed by the Consensus study (29, 30). In the present study, we did not find a favorable prognosis for patients with luminal-papillary subtype. Consistent with our results, an independent study with RC-treated MIBC patients could not confirm the favorable prognosis for the luminal-papillary subtype (46).

In addition to molecular subtypes, we investigated the prognostic values of different molecular signatures in the MIBC cohort of 100 fresh-frozen tumor samples. Our results revealed that stromal signature scores (genes expressed by the stromal cells), such as ECM, immune, and p53, were associated with improved OS and CSS. On the contrary, tumor intrinsic signatures (genes expressed by the tumor cells), such as luminal, basal, and squamous signatures showed no association with survival. Among the tumor

intrinsic factors, only the neuronal signature score influenced survival, which is consistent with the poor prognosis found for the neuronal molecular subtype. In accordance with our results, MIBC tumors with high numbers of tumor-infiltrating lymphocytes (inflamed tumors) showed better CSS compared to uninflamed tumors (47). Moreover, the lymphocyte infiltration was associated with molecular subtypes; the basal subtypes showed the highest lymphocyte infiltration, followed by the luminal-infiltrated subtype (47). Accordingly, the TCGA basal/squamous subtype also exhibited a high level of immune cell infiltration (29). A further study reported that MIBC tumors with higher infiltration of $CD8^+$ cytotoxic T cells and natural killer cells had better survival outcomes (48). In conclusion, the ECM, immune, and p53 signatures seem to influence patients' prognosis, thus the identification of smaller molecular subtypes with high stromal and immune cell infiltration is clinically important.

Routine histological tumor evaluation applies FFPE tumor samples, therefore this type of material is widely available for retrospective clinical research other than fresh-frozen tumor samples, which requires prospective and complicated sample logistics. Therefore, we aimed to transfer our rule set-based classifier method to routinely available FFPE samples. However, according to our technical analyses RNA samples purified from FFPE tissues frequently provided invalid results by the RT-qPCR method. Therefore, we decided to transfer gene expression analysis to the NanoString nCounter platform, which provided usable results also in those cases when RT-qPCR did not. As part of the optimization process, the panel was reduced from 68 to 48 genes, which required a respective adjustment of the rule sets. After this gene number reduction and rule set adjustment, our updated classifier method achieved similar or higher overlaps with the original transcriptome-based classifications than the previously used 68-gene marker set. Importantly, the 48-gene classifier method reached higher overlap with the LundTax transcriptome-based classification, than the 68-gene classifier. This result is important, as we plan to perform IHC-based molecular classification on our institutional cohort using the LundTax IHC classifier. Thereby, the LundTax subtypes identified by the gene expression-based and IHC-based classifiers will be directly comparable in the same samples.

By using the updated 48-gene classifier, we examined the chemotherapy predictive values of molecular subtypes. According to literature data, the p53-like subtype

(MDA) is associated with chemotherapy resistance (25), while Seiler *et al.* found that only the basal subtype (as identified by the GSC classifier) benefits from a NAC by an OS benefit, however authors did not present data on the important and less biased endpoint of pathological complete response (pCR) (26). In addition, a recent study using the GSC classifier could only partly confirm the higher chemotherapy sensitivity of the basal subtype. Authors separated luminal, luminal infiltrated, basal, and claudin-low subtypes, which were merged in two groups; of "luminal" and "non-luminal" subgroups. The non-luminal group included the basal, claudin-low, and surprisingly also the luminal infiltrated subtypes. As a result, they described those patients with non-luminal tumors showed significantly longer OS after NAC compared to patients treated by upfront RC alone. However, a similar survival outcome was observed in patients with luminal tumors with and without NAC treatment (49). The Consensus study, which reanalyzed the gene expression results of previously published datasets containing a total number of 1750 MIBC samples and defined the Consensus classification system, found no NAC predictive value for any of the subtypes (30). In contrast to the above results, a recent paper by Taber *et al.* divided patients into basal and non-basal subgroups and found that patients with non-basal tumors (mainly containing luminal subtypes) benefited from salvage platinum-based chemotherapy, while basal subtypes did not (50). In accordance with these results Sjödahl *et al.* examining the therapy predictive value of molecular subtypes by the LundTax classifier in a NAC-treated *vs.* upfront RC-treated patients found that tumors with luminal subtypes (such as the genomically unstable and urothelial-like subtypes) had significantly higher pCR rates compared to basal subtypes, which was consistent with the survival outcomes (28). Overall, the above presented literature data seem to be contradictory, however, a direct comparison of results may be difficult due to differences in chemotherapy setting (neoadjuvant or postoperative) or study endpoints (OS or pCR), and the applied subtype classification systems (MDA, LundTax, TCGA, GSC, Consensus).

Our present study is the first that assessed the platinum-predictive value of molecular subtypes (TCGA, MDA, LundTax and Consensus) in the adjuvant chemotherapy setting. We included two MIBC cohorts both with a guideline-based recommendation for adjuvant chemotherapy. The "chemo cohort" received platinum-based chemotherapy within 90 days after RC, while the "non-chemo cohort" was treated

only with RC without postoperative chemotherapy. Tumor samples were classified into molecular subtypes using our 48-gene panel-based classifier of the TCGA, MDA, LundTax, and Consensus classification systems. Then the therapy predictive values of distinct molecular subtypes were examined by comparing patients' OS between the chemotherapy-treated and non-treated patients within each molecular subtype. Our results showed that patients with the luminal-papillary subtype (according to TCGA and Consensus classifications), and those with the urothelial-like subtype (according to LundTax classification) may benefit from adjuvant chemotherapy. In contrast, basal tumors (according to each classification system) did not benefit from the administration of adjuvant chemotherapy. These results are in line with those of published by Sjödahl *et al.* as well as by Taber *et al.*, showing that rather luminal than basal subtypes are associated with platinum sensitivity in the adjuvant chemotherapy setting (28, 50).

A further aim of the present work was to test the chemotherapy predictive value of 12 single and potentially platinum-predictive genes. Some of these 12 genes were selected based on our preliminary results; *APOBECs, CLDN4, HMGA2, MKI67,* and *TOP2A* (unpublished data). Further three genes were selected according to formerly published data by Als *et al.*, who performed global gene expression profiling of tumor samples from platinum treated BC patients and identified *BIRC5, BSG, and HMGA2* as platinum predictive genes (13). In a subsequent IHC study, we were able to validate the therapy predictive value of *BIRC5* (protein name: Survivin), *BSG* (protein name: Emmprin), and *HMGA2* (15). *CDK12, ERCC1,* and *MMP7* were also selected based on literature data (17, 51, 52). The so selected 12 genes were measured in our institutional cohort (chemo *vs.* non-chemo) using the NanoString method and those genes with confirmed chemotherapy predictive values were further investigated in an independent dataset with NAC and RC-treated patients (Lund cohorts) (28, 46). According to the analysis of our institutional cohorts, high *APOBEC3G, CLDN4,* and *ERCC1* expressions and low *BIRC5, HMGA2,* and *MKI67* expressions were associated with significantly improved survival in the chemo cohort, but not in the non-chemo cohort. The validation analysis on the external Lund datasets confirmed the chemotherapy predictive values of *APOBEC3G, CLDN4,* and *BIRC5* in terms of OS. In addition, high *APOBEC3G* expression was associated with higher rates of pCR.

Claudin-4 (CLDN4) is a component of tight junction proteins, and its high expression was associated with local invasion, LN and distant metastasis, and pathological stage in chemo-naïve BC patients. In addition, the combination of CLDN4 antibody and cisplatin decreased the growth of tumors derived from subcutaneously inoculated T24 BC cells in mouse models (53), which results are inconsistent with the outcome of our analysis. In ovarian cancer cell lines, consistent with our results, the knockdown of *CLDN4* increased the resistance to cisplatin (54). To reveal the relation between chemotherapy efficacy and CLDN4, further immunohistochemical analysis of chemotherapy-treated tumor tissues and functional experiments on cisplatin sensitive and resistant BC cell lines are needed.

Survivin is an apoptosis inhibitor. Its enhanced expression may help to avoid therapy-induced cell death of tumor cells and thereby may contribute to therapy resistance (13). In a former study, we confirmed the association between a strong Survivin immunostaining and shorter survival in chemotherapy-treated BC patients (15). In the present study, we found that a high gene expression level of *Survivin*, similar to the protein level results, is associated with inferior survival after adjuvant chemotherapy.

In the present study, *APOBEC3G* was identified as platinum predictive marker in the adjuvant chemotherapy setting and its predictive value could be confirmed in the neoadjuvant setting as well. Furthermore, its elevated expression was associated with significantly higher pCR. *APOBEC3G* gene codes a cytidine deaminase, which has an important role in innate antiviral response. Expression analyses of *APOBEC3G* in various tumor types revealed a heterogeneous pattern, while no data are available for BC, and only one study assessed the expression of *APOBEC3G* expression in urothelial cancer cell lines (55). In colorectal cancer, positive *APOBEC3G* expression was suggested to be mechanistically involved in the formation of liver metastasis and was associated with a worse prognosis (56). In contrast, an independent study reported that high APOBEC3G protein expression is able to reduce the migration ability of human HCC cell line, Hep 3B (57). In melanoma patients, high *APOBEC3G* gene and protein expressions were found to be elevated in tumor compared to benign tissue and its higher expression levels were associated with more favorable overall and recurrence-free survival. Furthermore, high *APOBEC3G* expression was associated with higher immune cell infiltration (58). Based on our results, further analysis is required to reveal the mechanistic role of

APOBEC3G in chemotherapy response, however, the IHC-based separation of different APOBEC proteins from each other represents a major challenge (59).

The use of serum markers for chemotherapy prediction could also be easily integrated into the daily clinical routine. Based on former analyses and literature data, we selected SDC1 and MMP7 for measurement in baseline serum samples of chemotherapy-treated MIBC patients.

SDC1 is a transmembrane heparan sulfate proteoglycan, which is predominantly expressed in the epithelial cells. The members of the syndecan protein family are involved in cell signaling and cytoskeletal organization. SDC1 tissue expression, especially its intracellular localization was proved to be associated with patients' prognosis in MIBC (60). Higher serum SDC1 levels were observed in patients with high-stage and high-grade tumors and were associated with the presence of metastasis (60). In addition, a shift in the intracellular localization of SDC1 from the membrane to the cytoplasm has been observed during the progression of BC (60, 61). This phenomenon might be associated with the shedding of the extracellular domain of SDC1. The shedded extracellular domain of SDC1 can be detected in patients' serum samples. Yu *et al.* described a significantly higher expression of SDC1 in cisplatin resistant hepatic carcinoma cells (HepG2) compared to sensitive cell lines (38). In line with these results, a high stromal SDC1 expression was associated with higher tumor-specific mortality in patients with oral squamous carcinoma who received NAC (62). These results led us to measure the pretreatment serum levels of SDC1 in BC patients who receive cisplatin-based chemotherapy. We found that higher SDC1 serum levels independently correlating with shorter OS. On the other hand, we found no correlation between membranous or cytoplasmatic localization of SDC1 and OS of platinum-treated BC patients. A recent study by Seiler *et al*. reported that the changes of glycosaminoglycan chains of SDC1 may also influence BC patients' chemotherapy sensitivity (63). Therefore, further analyses are needed to reveal the potential mechanistic involvement of SDC1 in platinum resistance to clarify, whether high SDC1 serum and/or protein expressions are predictive or rather prognostic in BC.

MMP7 is a member of the matrix metalloproteinases enzyme family, which has been proved to be associated with the degradation of extracellular matrix (ECM) components, and thereby linked to tumor invasion and migration (64). In our previous

work, MMP7 tissue gene expression was significantly higher in MIBCs compared to NMIBCs, with the highest levels in metastatic BC patients. Accordingly, high serum MMP7 levels were associated with LN positivity and shorter overall, disease-specific and metastases-free survival (65). Furthermore, MMP7 was identified as a chemotherapy predictive marker by comparative transcript profiling analysis in cisplatin sensitive versus resistant head-and-neck squamous cell carcinoma cell lines (39). High MMP7 tissue protein expression was correlated with poor treatment response and shorter OS in non-small cell lung cancer patients who underwent platinum chemotherapy (66, 67). Similar results were found in progressed prostate cancer, where high baseline MMP7 serum levels were associated with shorter OS in patients who underwent docetaxel chemotherapy (68). The above results led us to examine the possible association between baseline serum MMP7 levels and OS in platinum-treated MIBC patients. Our results identified high pretreatment serum MMP7 levels to be independently associated with shorter OS in platinum treated MIBC patients. These results were then also confirmed in MIBC tissues, as strong MMP7 immunostainings were associated with a worse OS in platinum treated BC patients. However, our *in vitro* knockout analyses were not able to confirm the functional involvement of MMP7 in platinum resistance of BC cells. Further research needs to clarify whether MMP7 is a prognostic or therapy predictive marker in BC. However, the negative results of our *in vitro* analyses suggest the MMP7 is rather a prognostic than a predictive marker.

Members of the MMP family are involved in many processes, including ECM degradation, thereby tumor invasion and migration, as well as tumor angiogenesis, cell proliferation, and even apoptosis. Some MMP proteins, including MMP7, are able to cleave the extracellular domains of other proteins. Cleavage of the extracellular domain of the epithelial marker E-cadherin reduces the adhesion capacity of the cell and contributes to cell motility. On the other hand, MMP7 can also cleave the Fas receptor and ligand from the cell surface, thereby inhibiting apoptosis (69). Based on these, we assumed the MMP7 can cleave the extracellular domain of SDC1 as well. Thus, we correlated the serum levels of both proteins with each other and found a significant positive correlation between the proteins.

Based on the present study conducted on retrospective cohorts of patients with muscle-invasive bladder cancer, the following novel findings can be reported:

1) Tumors can be classified into different molecular subtypes using a reduced gene panel-based assays. RT-qPCR and NanoString-based gene expression analyses provide a more cost-effective and simpler method to determine molecular subtypes. The newly established, gene panel-based expression assay has also been optimized for the analysis of FFPE samples, which are the most commonly available specimens in clinicopathological diagnostics.
2) The determined molecular subtypes have prognostic value; patients with neural subtypes show poor outcomes.
3) The determined molecular subtypes have chemotherapy-predictive value; patients with luminal-papillary subtypes (TCGA and Consensus classifications) and urothelial subtypes (Lund Taxonomy) benefit from adjuvant chemotherapy.
4) Single genes may predict patients' chemotherapy response rates. High *APOBEC3G* gene expression is associated with longer overall survival in patients receiving adjuvant chemotherapy, compared to patients with a chemotherapy indication who were treated solely with radical cystectomy. Additionally, patients with high APOBEC3G expression demonstrated inferior pathological complete response rates in a cohort treated with neoadjuvant chemotherapy.
5) Serum markers for chemotherapy prediction can be easily integrated into routine clinical practice. High serum levels of SDC1 and MMP7 were associated with shorter overall survival in a cohort of patients treated with postoperative chemotherapy.
6) The tissue expression of MMP7 may be used to select patients for postoperative chemotherapy treatment.

Conclusions

In the present work, we aimed to develop a gene panel-based classifier method, which can be applied to a routine-compatible analytical platform and to provide robust results from low quality FFPE tissue samples as well. Our classifier method was able to accurately reproduce the most widely used mRNA-based classification systems (TCGA, MDA, LundTax, Consensus). Our 68-gene classifier method was tested on frozen tissue samples by using RT-qPCR analysis. In accordance with the published literature, we found that patients with neuronal and luminal subtypes had the poorest prognosis, while the favorable prognosis of luminal-papillary tumors could not be confirmed. In a further step, we optimized and reduced our panel to 48 genes and assessed the predictive value of molecular subtype classification for the first time in the context of adjuvant platinum therapy. We found that patients with luminal-papillary (according to TCGA and Consensus classifiers), and urothelial-like subtypes (according to LundTax classifier) benefited from adjuvant chemotherapy, while in contrast those patients with basal tumors did not.

In addition, we assessed 12 potential chemotherapy predictive markers and confirmed the platinum predictive value of *APOBEC3G*, *CLDN4*, and *BIRC5*. In addition, *APOBEC3G* expression was significantly associated also with the pathological complete response rates in the neoadjuvant setting.

Finally, we identified high pretreatment levels of SDC1 and MMP7 as independent predictors of poor survival in platinum-treated MIBC patients.

Our results suggest that determination of molecular subtypes and *APOBEC3G*, *CLDN4*, and *BIRC5* gene expressions as well as SDC1 and MMP7 serum concentrations may help to improve therapeutic decision-making in MIBC. However, prospective studies are needed to confirm our results before their implementation into the clinical routine.

6. Summary

Recently, both prognostic and predictive values of distinct molecular BC subtypes have been revealed. In the future, molecular subtypes may play a crucial role in the therapeutic decision-making of patients with MIBC. Current molecular subtyping is based on transcriptome sequencing, which is associated with high demands of input samples, technical complexity, and high costs. This technical barrier largely hindered the widespread adoption of the molecular classification in the daily clinical routine. Therefore, we aimed to develop a simple gene panel-based classification method that can identify molecular subtypes according to TCGA, MDA, LundTax, and Consensus classifications. To this aim, we developed a rule set-based classifier method, which has been applied to fresh-frozen MIBC samples by measuring the gene expression of 68 genes using RT-qPCR. Then, we classified our institutional cohort of 100 MIBC samples into molecular subtypes and examined their prognostic values. In line with the original studies, patients with neuronal subtypes had the worst survival. In addition, we found that strong extracellular matrix and immune cell signatures were associated with improved survival, suggesting that the tumor microenvironment play an important role in tumor progression. As a next step, the rule set-based classifier method was optimized (the marker set was reduced from 68 to 48 genes) and the analytical platform was transferred to the NanoString nCounter technology to enable the analysis of FFPE tumor samples. We then applied our updated rule-set-based classifier to our institutional MIBC cohort, which included adjuvant chemotherapy-treated and non-treated patients. Luminal-papillary subtype (TCGA, Consensus), and urothelial-like subtype (LundTax) were associated with longer survival in the chemo cohort compared to non-chemo cohort. Patients with luminal papillary or urothelial-like subtypes may benefit from adjuvant chemotherapy.

Expression levels of 12 genes with potential chemotherapy predictive value were evaluated in our chemo and non-chemo MIBC cohorts. Patients with high levels of *APOBEC3G* and *CLDN4* as well as with low levels of *BIRC5* showed improved survival in the chemo, but not in the non-chemo cohort. These results could be confirmed in an external dataset. In addition, high *APOBEC3G* expression correlated with the significantly higher pCR rates in patients who received NAC.

High baseline serum levels of SDC1 and MMP7 were associated with inferior survival outcomes in MIBC patients who received platinum-based chemotherapy.

7. References

1. Bray F, Ferlay J, Soerjomataram I. Global Cancer Statistics 2018 : GLOBOCAN Estimates of Incidence and Mortality Worldwide for 36 Cancers in 185 Countries. A Cancer J Clin. 2018;68(6):394–424.
2. Kásler M, Ottó S, Kenessey I. A rákmorbiditás és-mortalitás jelenlegi helyzete a Nemzeti Rákregiszter tükrében. Orv Hetil. 2017;158(3):84–9.
3. Leiblich A, Bryant RJ, Mccormick R, Crew J. The management of non-muscle-invasive bladder cancer : A comparison of European and UK guidelines. J Clin Urol. 2018;11:144–8.
4. Lerner SP, Robertson AG. Molecular Subtypes of Non-muscle Invasive Bladder Cancer. Cancer Cell. 2016;30(1):1–3.
5. Minoli M, Kiener M, Thalmann GN, Julio MK De, Seiler R. Evolution of urothelial bladder cancer in the context of molecular classifications. Int J Mol Sci. 2020;21(16):1–25.
6. Felsenstein KM, Theodorescu D. Precision medicine for urothelial. Nat Rev Urol. 2017;15:92–111.
7. Witjes JA, Bruins HM, Cathomas R, Compérat EM, Cowan NC, Gakis G, Hernández V, Linares Espinós E, Lorch A, Neuzillet Y, Rouanne M, Thalmann GN, Veskimäe E, Ribal MJ, van der Heijden AG. European Association of Urology Guidelines on Muscle-invasive and Metastatic Bladder Cancer: Summary of the 2020 Guidelines. Eur Urol. 2021;79:82–104.
8. Leow JJ, Martin-Doyle W, Rajagopal PS, Patel CG, Anderson EM, Rothman AT, Cote RJ, Urun Y, Chang SL, Choueiri TK, Bellmunt J. Adjuvant chemotherapy for invasive bladder cancer: A 2013 updated systematic review and meta-analysis of randomized trials. Eur Urol. 2014;66(1):42–54.
9. Natale RB. Adjuvant and neoadjuvant chemotherapy for invasive bladder cancer. Curr Oncol Rep. 2000;2(5):386–93.
10. Powles T, Bellmunt J, Comperat E, De Santis M, Huddart R, Loriot Y, Necchi A, Valderrama BP, Ravaud A, Shariat SF, Szabados B, van der Heijden MS, Gillessen S. Bladder cancer: ESMO Clinical Practice Guideline for diagnosis, treatment and follow-up ☆. Ann Oncol. 2022;33(3):244–58.

11. Rosenberg JE, Hoffman-Censits J, Powles T, van der Heijden MS. Atezolizumab in patients with locally advanced and metastatic urothelial carcinoma who have progressed following treatment with platinum-based chemotherapy: a single arm, phase 2 trial Jonathan. Lancet. 2016;387(10031):1909–20.
12. Powles T, Park SH, Voog E, Caserta C, Valderrama BP, Gurney H, Kalofonos H, Radulović S, Demey W, Ullén A, Loriot Y, Sridhar SS, Tsuchiya N, Kopyltsov E, Sternberg CN, Bellmunt J, Aragon-Ching JB, Petrylak DP, Laliberte R, Wang J, Huang B, Davis C, Fowst C, Costa N, Blake-Haskins JA, di Pietro A, Grivas P. Avelumab Maintenance Therapy for Advanced or Metastatic Urothelial Carcinoma. N Engl J Med. 2020;383(13):1218–30.
13. Als AB, Dyrskjøt L, Von Der Maase H, Koed K, Mansilla F, Toldbod HE, Jensen JL, Ulhøi BP, Sengeløv L, Jensen KM, Orntoft TF. Emmprin and survivin predict response and survival following cisplatin-containing chemotherapy in patients with advanced bladder cancer. Clin Cancer Res. 2007;13(15):4407–14.
14. Krafft U, Tschirdewahn S, Hess J, Harke NN, Hadaschik BA, Nyirády P, Szendröi A, Szücs M, Módos O, Olah C, Székely E, Reis H, Szarvas T. STIP1 Tissue Expression Is Associated with Survival in Chemotherapy-Treated Bladder Cancer Patients. Pathol Oncol Res. 2020;26(2):1243–9.
15. Krafft U, Tschirdewahn S, Hess J, Harke NN, Hadaschik B, Olah C, Krege S, Nyirády P, Szendröi A, Szücs M, Módos O, Székely E, Reis H, Szarvas T. Validation of survivin and HMGA2 as biomarkers for cisplatin resistance in bladder cancer. Urol Oncol Semin Orig Investig. 2019;37(11):810.e7-810.e15.
16. Ozcan MF, Dizdar O, Dincer N, Balci S, Guler G, Gok B, Pektas G, Seker MM, Aksoy S, Arslan C, Yalcin S, Balbay MD. Low ERCC1 expression is associated with prolonged survival in patients with bladder cancer receiving platinum-based neoadjuvant chemotherapy. Urol Oncol Semin Orig Investig. 2013;31(8):1709–15.
17. Sun JM, Sung JY, Park SH, Kwon GY, Jeong BC, Seo SI, Jeon SS, Lee HM, Jo J, Choi HY, Lim HY. ERCC1 as a biomarker for bladder cancer patients likely to benefit from adjuvant chemotherapy. *BMC Cancer*. 2012;12:187. Published 2012 May 22. doi:10.1186/1471-2407-12-187.

18. Allen EM Van, Mouw KW, Kim P, Iyer G, Wagle N, Al-ahmadie H, Zhu C, Ostrovnaya I, Kryukov GV, O'Connor KW, Sfakianos J, Garcia-Grossman I, Kim J, Guancial EA, Bambury R, Bahl S, Gupta N, Farlow D, Qu A, Signoretti S, Barletta JA, Reuter V, Boehm J, Lawrence M, Getz G, Kantoff P, Bochner BH, Choueiri TK, Bajorin DF, Solit DB, Gabriel S, D'Andrea A, Garraway LA, Rosenberg JE. Somatic ERCC2 mutations correlate with cisplatin sensitivity in muscle-invasive urothelial carcinoma. Am Assoc Cancer Res. 2014;4:1140–53.
19. Plimack ER, Dunbrack RL, Brennan TA, Andrake MD, Zhou Y, Serebriiskii IG, Slifker M, Alpaugh K, Dulaimi E, Palma N, Hoffman-Censits J, Bilusic M, Wong YN, Kutikov A, Viterbo R, Greenberg RE, Chen DY, Lallas CD, Trabulsi EJ, Yelensky R, McConkey DJ, Miller VA, Golemis EA, Ross EA. Platinum Priority – Bladder Cancer Defects in DNA Repair Genes Predict Response to Neoadjuvant Cisplatin-based Chemotherapy in Muscle-invasive Bladder Cancer. Eur Urol. 2015;68(6):959–67.
20. Bellmunt J, Powles T, Vogelzang NJ. A review on the evolution of PD-1/PD-L1 immunotherapy for bladder cancer: The future is now. Cancer Treat Rev. 2017;54:58–67.
21. Suzman DL, Agrawal S, Ning Y, Maher VE, Fernandes LL, Karuri S, Tang S, Sridhara R, Schroeder J, Goldberg KB, Ibrahim A, McKee AE, Pazdur R, Beaver JA. FDA Approval Summary: Atezolizumab or Pembrolizumab for the Treatment of Patients with Advanced Urothelial Carcinoma Ineligible for Cisplatin-Containing Chemotherapy. Oncologist. 2019;24(4):563–9.
22. Sharma P, Retz M, Siefker-Radtke A, Baron A, Necchi A, Bedke J, Plimack ER, Vaena D, Grimm MO, Bracarda S, Arranz JÁ, Pal S, Ohyama C, Saci A, Qu X, Lambert A, Krishnan S, Azrilevich A, Galsky MD. Nivolumab in metastatic urothelial carcinoma after platinum therapy (CheckMate 275): a multicentre, single-arm, phase 2 trial. Lancet Oncol. 2017;18(3):312–22.
23. Goswami S, Chen Y, Anandhan S, Szabo PM, Basu S, Blando JM, Liu W, Zhang J, Natarajan SM, Xiong L, Guan B, Yadav SS, Saci A, Allison JP, Galsky MD, Sharma P. ARID1A mutation plus CXCL13 expression act as combinatorial biomarkers to predict responses to immune checkpoint therapy in mUCC. Sci Transl Med. 2020;12(548).

24. Damrauer JS, Hoadley KA, Chism DD, Fan C, Tiganelli CJ. Intrinsic subtypes of high-grade bladder cancer reflect the hallmarks of breast cancer biology. Proc Natl Acad Sci. 2014;111(8):3110–5.
25. Choi W, Porten S, Kim S, Willis D, Plimack ER, Hoffman-Censits J, Roth B, Cheng T, Tran M, Lee IL, Melquist J, Bondaruk J, Majewski T, Zhang S, Pretzsch S, Baggerly K, Siefker-Radtke A, Czerniak B, Dinney CP, McConkey DJ. Identification of Distinct Basal and Luminal Subtypes of Muscle-Invasive Bladder Cancer with Different Sensitivities to Frontline Chemotherapy. Cancer Cell. 2014;25(2):152–65.
26. Seiler R, Ashab HAD, Erho N, van Rhijn BWG, Winters B, Douglas J, Van Kessel KE, Fransen van de Putte EE, Sommerlad M, Wang NQ, Choeurng V, Gibb EA, Palmer-Aronsten B, Lam LL, Buerki C, Davicioni E, Sjödahl G, Kardos J, Hoadley KA, Lerner SP, McConkey DJ, Choi W, Kim WY, Kiss B, Thalmann GN, Todenhöfer T, Crabb SJ, North S, Zwarthoff EC, Boormans JL, Wright J, Dall'Era M, van der Heijden MS, Black PC. Impact of Molecular Subtypes in Muscle-invasive Bladder Cancer on Predicting Response and Survival after Neoadjuvant Chemotherapy. Eur Urol. 2017;72:544–54.
27. Sjödahl G, Eriksson P, Liedberg F, Höglund M. Molecular classification of urothelial carcinoma: global mRNA classification versus tumour-cell phenotype classification. J Pathol. 2017;242(1):113–25.
28. Sjödahl G, Abrahamsson J, Holmsten K, Bernardo C, Chebil G, Eriksson P, Johansson I, Kollberg P, Lindh C, Lövgren K, Marzouka NA, Olsson H, Höglund M, Ullén A, Liedberg F. Different Responses to Neoadjuvant Chemotherapy in Urothelial Carcinoma Molecular Subtypes. Eur Urol. 2021;S0302-2838(21)02138-2.

29. Robertson AG, Kim J, Al-Ahmadie H, Bellmunt J, Guo G, Cherniack AD, Hinoue T, Laird PW, Hoadley KA, Akbani R, Castro MAA, Gibb EA, Kanchi RS, Gordenin DA, Shukla SA, Sanchez-Vega F, Hansel DE, Czerniak BA, Reuter VE, Su X, de Sa Carvalho B, Chagas VS, Mungall KL, Sadeghi S, Pedamallu CS, Lu Y, Klimczak LJ, Zhang J, Choo C, Ojesina AI, Bullman S, Leraas KM, Lichtenberg TM, Wu CJ, Schultz N, Getz G, Meyerson M, Mills GB, McConkey DJ; TCGA Research Network; Weinstein JN, Kwiatkowski DJ, Lerner SP.Comprehensive Molecular Characterization of Muscle-Invasive Bladder Cancer. Cell. 2017;171(3):540-556.e25.

30. Kamoun A, de Reyniès A, Allory Y, Sjödahl G, Robertson AG, Seiler R, Hoadley KA, Groeneveld CS, Al-Ahmadie H, Choi W, Castro MAA, Fontugne J, Eriksson P, Mo Q, Kardos J, Zlotta A, Hartmann A, Dinney CP, Bellmunt J, Powles T, Malats N, Chan KS, Kim WY, McConkey DJ, Black PC, Dyrskjøt L, Höglund M, Lerner SP, Real FX, Radvanyi F; Bladder Cancer Molecular Taxonomy Group. A Consensus Molecular Classification of Muscle-invasive Bladder Cancer. Eur Urol. 2020;77(4):420–33.

31. Font A, Domènech M, Benítez R, Rava M, Marqués M, Ramírez JL, Pineda S, Domínguez-Rodríguez S, Gago JL, Badal J, Carrato C, López H, Quer A, Castellano D, Malats N, Real FX. Immunohistochemistry-based taxonomical classification of bladder cancer predicts response to neoadjuvant chemotherapy. Cancers (Basel). 2020;12(7):1784.

32. Ikeda J, Ohe C. Comprehensive pathological assessment of histological subtypes , molecular subtypes based on immunohistochemistry , and tumor - associated immune cell status in muscle - invasive bladder cancer. Pathol Int. 2020;71(3):173–82.

33. Guo CC, Bondaruk J, Yao H, Wang Z, Zhang L, Lee S, Lee JG, Cogdell D, Zhang M, Yang G, Dadhania V, Choi W, Wei P, Gao J, Theodorescu D, Logothetis C, Dinney C, Kimmel M, Weinstein JN, McConkey DJ, Czerniak B. Assessment of Luminal and Basal Phenotypes in Bladder Cancer. Sci Rep. 2020;10(1):9743.

34. Sjödahl G. Molecular Subtype Profiling of Urothelial Carcinoma Using a Subtype-Specific Immunohistochemistry Panel. *Methods Mol Biol*. 2018;1655:53-64.

35. Aine M, Eriksson P, Liedberg F, Sjödahl G, Höglund M. Biological determinants of bladder cancer gene expression subtypes. Sci Rep. 2015;5:10957.
36. Grivas P, Bismar TA, Alva AS, Huang HC, Liu Y, Seiler R, Alimohamed N, Cheng L, Hyndman ME, Dabbas B, Black PC, Davicioni E, Wright JL, Ornstein MC, Mian OY, Kaimakliotis HZ, Gibb EA, Lotan Y. Validation of a neuroendocrine-like classifier confirms poor outcomes in patients with bladder cancer treated with cisplatin-based neoadjuvant chemotherapy. Urol Oncol Semin Orig Investig. 2019;38(4):262–8.
37. Da Costa JB, Gibb EA, Bivalacqua TJ, Liu Y, Zarni Oo H, Miyamoto DT, Alshalalfa M, Davicioni E, Wright J, Dall'Era MA, Douglas J, Boormans JL, Van der Heijden MS, Wu CL, van Rhijn BWG, Gupta S, Grivas P, Mouw KW, Murugan P, Fazli L, Ra S, Konety BR, Seiler R, Daneshmand S, Mian OY, Efstathiou JA, Lotan Y, Black PC. Molecular characterization of neuroendocrinelike bladder cancer. Clin Cancer Res. 2019;25(13):3908–20.
38. Yu L, Xu H, Zhang S, Chen J, Yu Z. SDC1 promotes cisplatin resistance in hepatic carcinoma cells via PI3K-AKT pathway. Hum Cell. 2020;(0123456789).
39. Ansell A, Jerhammar F, Ceder R, Grafström R, Grénman R, Roberg K. Matrix metalloproteinase-7 and -13 expression associate to cisplatin resistance in head and neck cancer cell lines. Oral Oncol. 2009;45(10):866–71.
40. Wang X, Zuo D, Chen Y, Li W, Liu R, He Y, Ren L, Zhou L, Deng T, Wang X, Ying G, Ba Y. Shed Syndecan-1 is involved in chemotherapy resistance via the EGFR pathway in colorectal cancer. Br J Cancer. 2014;111(10):1965–76.
41. Rinaldetti S, Rempel E, Worst TS, Eckstein M, Steidler A, Weiss CA, Bolenz C, Hartmann A, Erben P. Subclassification, survival prediction and drug target analyses of chemotherapy-naïve muscle-invasive bladder cancer with a molecular screening. Oncotarget. 2018;9(40):25935–45.
42. Kardos J, Rose TL, Manocha U, Wobker SE, Damrauer JS, Bivalaqua TJ, Kates M, Moore KJ, Parker JS, Kim WY. Development and validation of a NanoString BASE47 bladder cancer gene classifier. PLoS One. 2020;15(12):e0243935.

43. Morera DS, Hasanali SL, Belew D, Ghosh S, Klaassen Z, Jordan AR, Wang J, Terris MK, Bollag RJ, Merseburger AS, Stenzl A, Soloway MS, Lokeshwar VB. Clinical Parameters Outperform Molecular Subtypes for Predicting Outcome in Bladder Cancer: Results from Multiple Cohorts, Including TCGA. J Urol. 2020;203(1):62–72.
44. Höglund M, Bernardo C, Sjödahl G, Eriksson P, Axelson H, Liedberg F. The Lund Taxonomy for Bladder Cancer Classification – From Gene Expression Clustering to Cancer Cell Molecular Phenotypes, and Back Again. J Pathol. 2023;259(4):369–75.
45. Kim J, Kwiatkowski D, McConkey DJ, Meeks JJ, Freeman SS, Bellmunt J, Getz G, Lerner SP. The Cancer Genome Atlas Expression Subtypes Stratify Response to Checkpoint Inhibition in Advanced Urothelial Cancer and Identify a Subset of Patients with High Survival Probability. Eur Urol. 2019;75(6):961–4.
46. Kollberg P, Chebil G, Eriksson P, Sjödahl G, Liedberg F. Molecular subtypes applied to a population-based modern cystectomy series do not predict cancer-specific survival. Urol Oncol Semin Orig Investig. 2019;37(10):791–9.
47. Pfannstiel C, Strissel PL, Chiappinelli KB, Sikic D, Wach S, Wirtz RM, Wullweber A, Taubert H, Breyer J, Otto W, Worst T, Burger M, Wullich B, Bolenz C, Fuhrich N, Geppert CI, Weyerer V, Stoehr R, Bertz S, Keck B, Erlmeier F, Erben P, Hartmann A, Strick R, Eckstein M; BRIDGE Consortium, Germany. The tumor immune microenvironment drives a prognostic relevance that correlates with bladder cancer subtypes. Cancer Immunol Res. 2019;7(6):923–38.
48. Fu H, Zhu Y, Wang Y, Liu Z, Zhang J, Xie H, et al. Identification and validation of stromal immunotype predict survival and benefit from adjuvant chemotherapy in patients with muscle-invasive bladder cancer. Clin Cancer Res. 2018;24(13):3069–78.
49. Lotan Y, de Jong J, Liu VYT, Bismar TA, Boorjian SA, Huang HC, Davicioni E, Mian OY, Wright JL, Necchi A, Dall'Era MA, Kaimakliotis HZ, Black PC, Gibb EA, Boormans JL. Patients With Muscle Invasive Bladder Cancer with Non-luminal Subtype Derive Greatest Benefit from Platinum Based Neoadjuvant Chemotherapy. J Urol. 2022; 207(3):541-550.

50. Taber A, Christensen E, Lamy P, Nordentoft I, Prip F, Lindskrog SV, Birkenkamp-Demtröder K, Okholm TLH, Knudsen M, Pedersen JS, Steiniche T, Agerbæk M, Jensen JB, Dyrskjøt L. Molecular correlates of cisplatin-based chemotherapy response in muscle invasive bladder cancer by integrated multi-omics analysis. Nat Commun. 2020;11:1–15.
51. Lui GYL, Grandori C, Kemp CJ. CDK12: An emerging therapeutic target for cancer. J Clin Pathol. 2018;71(11):957–62.
52. Szarvas T, Sevcenco S, Módos O, Keresztes D, Nyirády P, Csizmarik A, Ristl R, Puhr M, Hoffmann MJ, Niedworok C, Hadaschik B, Maj-Hes A, Shariat SF, Kramer G. Matrix metalloproteinase 7, soluble Fas and Fas ligand serum levels for predicting docetaxel resistance and survival in castration-resistant prostate cancer. BJU Int. 2018;122(4):695–704.
53. Kuwada M, Chihara Y, Lio Y, Li X, Nishiguchi Y, Fujiwara R, Sasaki T, Fujii K, Ohmori H, Fujimoto K, Kondoh M, Kuniyasu H. Pro-chemotherapeutic effects of antibody against extracellular domain of claudin-4 in bladder cancer. Cancer Lett. 2015;369:212–21.
54. Shang X, Lin X, Manorek G, Howell SB. Claudin-3 and claudin-4 regulate sensitivity to cisplatin by controlling expression of the copper and cisplatin influx transporter CTR1. Mol Pharmacol. 2013;83(1):85–94.
55. Vasudevan AAJ, Kreimer U, Schulz WA, Krikoni A, Schumann GG, Häussinger D, Münk C, Goering W. APOBEC3B activity is prevalent in urothelial carcinoma cells and only slightly affected by LINE-1 expression. Front Microbiol. 2018;9:1–17.
56. Lan H, Jin K, Gan M, Wen S, Bi T, Zhou S, Zhu N, Teng L, Yu W. APOBEC3G expression is correlated with poor prognosis in colon carcinoma patients with hepatic metastasis. Int J Clin Exp Med. 2014;7(3):665–72.
57. Chang LC, Kuo TY, Liu CW, Chen Y Sen, Lin HH, Wu PF. APOBEC3G exerts tumor suppressive effects in human hepatocellular carcinoma. Anticancer Drugs. 2014;25(4):456–61.
58. Han W, Xu J, Shen GL. Prognostic implication and functional annotations of APOBEC3G expression in patients with Melanoma. J Cancer. 2020;11:5245–56.

59. Vasudevan AAJ, Goering W, Häussinger D, Münk C. Detection of APOBEC3 Proteins and Catalytic Activity in Urothelial Carcinoma. In: Schulz WA, Hoffmann MJ, Niegisch G, editors. Methods in Molecular Biology. Humana Press, New York; 2018. p. 97–107.
60. Szarvas T, Reis H, Kramer G, Shariat SF, Vom Dorp F, Tschirdewahn S, Schmid KW, Kovalszky I, Rübben H. Enhanced stromal syndecan-1 expression is an independent risk factor for poor survival in bladder cancer. Hum Pathol. 2014;45(4):674–82.
61. Miyake M, Lawton A, Dai Y, Chang M, Mengual L, Alcaraz A, Goodison S, Rosser CJ. Clinical implications in the shift of syndecan-1 expression from the cell membrane to the cytoplasm in bladder cancer. BMC Cancer. 2014;14(86):1–7.
62. Ramani VC, Sanderson RD. Chemotherapy stimulates syndecan-1 shedding: A potentially negative effect of treatment that may promote tumor relapse. Matrix Biol. 2014;35:215–22.
63. Seiler R, Oo HZ, Tortora D, Clausen TM, Wang CK, Kumar G, Pereira MA, Ørum-Madsen MS, Agerbæk MØ, Gustavsson T, Nordmaj MA, Rich JR, Lallous N, Fazli L, Lee SS, Douglas J, Todenhöfer T, Esfandnia S, Battsogt D, Babcook JS, Al-Nakouzi N, Crabb SJ, Moskalev I, Kiss B, Davicioni E, Thalmann GN, Rennie PS, Black PC, Salanti A, Daugaard M. An Oncofetal Glycosaminoglycan Modification Provides Therapeutic Access to Cisplatin-resistant Bladder Cancer. Eur Urol. 2017;72(1):142–50.
64. Fingleton B, Vargo-Gogola T, Crawford HC, Matrisian LM. Matrilysin [MMP-7] expression selects for cells with reduced sensitivity to apoptosis. Neoplasia. 2001;3(6):459–68.
65. Szarvas T, Becker M, vom Dorp F, Gethmann C, Tötsch M, Bánkfalvi Á, Schmid KW, Romics I, Rübben H, Ergün S. Matrix metalloproteinase-7 as a marker of metastasis and predictor of poor survival in bladder cancer. Cancer Sci. 2010;101(5):1300–8.
66. Liu H, Zhang T, Li X, Huang J, Wu B, Huang X, Zhou Y, Zhu J, Hou J. Predictive value of MMP-7 expression for response to chemotherapy and survival in patients with non-small cell lung cancer. Cancer Sci. 2008;99(11):2185–92.

67. Huang Y, Yu H, Lei H, Xie C, Zhong Y. Matrix metalloproteinase 7 is a useful marker for 5-fluorouracil-based adjuvant chemotherapy in stage II and stage III colorectal cancer patients. Med Oncol. 2014;31(824):1–8.
68. Szarvas T, Csizmarik A, Váradi M, Fazekas T, Hüttl A, Nyirády P, Hadaschik B, Grünwald V, Tschirdewahn S, Shariat SF, Sevcenco S, Maj-Hes A, Kramer G. The prognostic value of serum MMP-7 levels in prostate cancer patients who received docetaxel, abiraterone, or enzalutamide therapy. Urol Oncol Semin Orig Investig. 39(5):296.e11-296.e19.
69. Szarvas T, Vom Dorp F, Ergün S, Rübben H. Matrix metalloproteinases and their clinical relevance in urinary bladder cancer. Nat Rev Urol. 2011;8(5):241–54.

8. Bibliography of the candidate's publications

Related to the thesis:

1. Szarvas T, Oláh C, Riesz P, Géczi L, Nyirády P. A húgyhólyag urothelialis daganatainak molekuláris alcsoportbeosztása és annak klinikai vonatkozásai [Molecular subtype classification of urothelial bladder cancer and its clinical relevance]. Orv Hetil. 2019 Oct;160(42):1647-1654. Hungarian. doi: 10.1556/650.2019.31559. **IF: 0.540**
2. Olah C, Tschirdewahn S, Hoffmann MJ, Krafft U, Hadaschik B, Nyirady P, Szendröi A, Módos O, Csizmarik A, Kovalszky I, Reis H, Szarvas T. Soluble Syndecan-1 Levels Are Associated with Survival in Platinum-Treated Bladder Cancer Patients. Diagnostics. 2020;10(11):864. doi: 10.3390/diagnostics10110864. **IF: 3.706**
3. Szarvas T, Hoffmann MJ, Olah C, Szekely E, Kiss A, Hess J, Tschirdewahn S, Hadaschik B, Grotheer V, Nyirady P, Csizmarik A, Varadi M, Reis H. MMP-7 Serum and Tissue Levels Are Associated with Poor Survival in Platinum-Treated Bladder Cancer Patients. Diagnostics (Basel). 2020 Dec 31;11(1):48. doi: 10.3390/diagnostics11010048. **IF: 3.706**
4. Olah C, Hahnen C, Nagy N, Musial J, Varadi M, Nyiro G, Gyorffy B, Hadaschik B, Rawitzer J, Ting S, Sjödahl G, Hoffmann MJ, Reis H, Szarvas T. A quantitative polymerase chain reaction based method for molecular subtype classification of urinary bladder cancer-Stromal gene expressions show higher prognostic values than intrinsic tumor genes. Int J Cancer. 2022 Mar 1;150(5):856-867. doi: 10.1002/ijc.33809. **IF: 7.316**
5. Olah C, Reis H, Hoffmann MJ, Mairinger F, Ting S, Hadaschik B, Krafft U, Grünwald V, Nyirady P, Varadi M, Győrffy B, Kiss A, Szekely E, Sjödahl G, Szarvas T. Predictive value of molecular subtypes and APOBEC3G for adjuvant chemotherapy in urothelial bladder cancer. Cancer Med. 2023 Mar;12(5):5222-5232. doi: 10.1002/cam4.5324. **IF: 4.711**
6. Koll FJ, Döring C, Olah C, Szarvas T, Köllermann J, Hoeh B, Chun FK, Reis H, Wild PJ. Optimizing identification of consensus molecular subtypes in muscle-invasive bladder cancer: a comparison of two sequencing methods and gene sets using FFPE specimens. BMC Cancer. 2023 Jun 4;23(1):504. doi: 10.1186/s12885-023-11016-9. **IF: 3.8**
7. Olah C, Szarvas T. A Panel-Based Method for the Reproduction of Distinct Molecular Subtype Classifications of Muscle-Invasive Urothelial Bladder Cancer. Methods Mol Biol. 2023;2684:27-43. doi: 10.1007/978-1-0716-3291-8_2. IF: **1.4**

Further publications not related to this thesis:

1. Szarvas T, Olah C, Reis H: Neoadjuvant cisplatin-based chemotherapy in "primary" and "secondary" muscle-invasive bladder cancer—is it a surrogate for molecular subtypes? Translational Cancer Research,2019;8:S176-S179. **IF: 0.918**
2. Szarvas T, Jardin-Watelet B, Bourgoin N, Hoffmann MJ, Nyirády P, Oláh C, Széll T, Csizmarik A, Hadaschik B, Reis H. High-soluble CGA levels are associated with poor survival in bladder cancer. Endocr Connect. 2019 May 1;8(5):625-633. doi: 10.1530/EC-19-0068. **IF: 2.592**
3. Krafft U, Tschirdewahn S, Hess J, Harke NN, Hadaschik B, Olah C, Krege S, Nyirády P, Szendröi A, Szücs M, Módos O, Székely E, Reis H, Szarvas T. Validation of survivin and HMGA2 as biomarkers for cisplatin resistance in bladder cancer. Urol Oncol. 2019 Nov;37(11):810.e7-810.e15. doi: 10.1016/j.urolonc.2019.04.015. **IF: 2.826**
4. Krafft U, Tschirdewahn S, Hess J, Harke NN, Hadaschik BA, Nyirády P, Szendröi A, Szücs M, Módos O, Olah C, Székely E, Reis H, Szarvas T. STIP1 Tissue Expression Is Associated with Survival in Chemotherapy-Treated Bladder Cancer Patients. Pathol Oncol Res. 2020 Apr;26(2):1243-1249. doi: 10.1007/s12253-019-00689-y. **IF: 3.201**
5. Nagy N, Reis H, Hadaschik B, Niedworok C, Módos O, Szendrői A, Bíró K, Hager T, Herold T, Ablat J, Black PC, Okon K, Tolkach Y, Csizmarik A, Oláh C, Keresztes D, Bremmer F, Gaisa NT, Kriegsmann J, Kovalszky I, Kiss A, Tímár J, Szász MA, Rink M, Fisch M, Nyirády P, Szarvas T. Prevalence of APC and PTEN Alterations in Urachal Cancer. Pathol Oncol Res. 2020 Oct;26(4):2773-2781. doi: 10.1007/s12253-020-00872-6. **IF: 3.201**
6. Oláh C, Váradi M, Horváth O, Nyirády P, Szarvas T. A béltartalom és a vizelet mikrobiom-összetételének onkológiai vonatkozásai [Oncological relevance of gut and urine microbiomes]. Orv Hetil. 2021;162(15):579-586. doi:10.1556/650.2021.32052. **IF: 0.707**
7. Krafft U, Olah C, Reis H, Kesch C, Darr C, Grünwald V, Tschirdewahn S, Hadaschik B, Horvath O, Kenessey I, Nyirady P, Varadi M, Modos O, Csizmarik A, Szarvas T. High Serum PD-L1 Levels Are Associated with Poor Survival in Urothelial Cancer Patients Treated with Chemotherapy and Immune Checkpoint Inhibitor Therapy. Cancers. 2021;13(11):2548. doi: 10.3390/cancers13112548. **IF: 6.575**
8. Kovács PT, Mayer T, Csizmarik A, Váradi M, Oláh C, Széles Á, Tschirdewahn S, Krafft U, Hadaschik B, Nyirády P, Riesz P, Szarvas T. Elevated Pre-Treatment Serum MMP-7 Levels Are Associated with the Presence of Metastasis and Poor Survival in Upper Tract Urothelial Carcinoma. Biomedicines. 2022 Mar 17;10(3):698. doi: 10.3390/biomedicines10030698. **IF: 4.757**

9. Széles Á, Kovács PT, Csizmarik A, Váradi M, Riesz P, Fazekas T, Váncsa S, Hegyi P, Oláh C, Tschirdewahn S, Darr C, Krafft U, Grünwald V, Hadaschik B, Horváth O, Nyirády P, Szarvas T. High Pretreatment Serum PD-L1 Levels Are Associated with Muscle Invasion and Shorter Survival in Upper Tract Urothelial Carcinoma. Biomedicines. 2022 Oct 13;10(10):2560. doi: 10.3390/biomedicines10102560**. IF: 4.757**

10. Tóth G, Sugár S, Pál D, Fügedi KD, Drahos L, Schlosser G, Oláh C, Reis H, Kovalszky I, Szarvas T, Turiák L. Glycosaminoglycan Analysis of FFPE Tissues from Prostate Cancer and Benign Prostate Hyperplasia Patients Reveals Altered Regulatory Functions and Independent Markers for Survival. Cancers. 2022;14(19):4867. doi: 10.3390/cancers14194867. **IF: 6.575**

11. Varadi M, Nagy N, Reis H, Hadaschik B, Niedworok C, Modos O, Szendroi A, Ablat J, Black PC, Keresztes D, Csizmarik A, Olah C, Gaisa NT, Kiss A, Timar J, Toth E, Csernak E, Gerstner A, Mittal V, Karkampouna S, Kruithof de Julio M, Gyorffy B, Bedics G, Rink M, Fisch M, Nyirady P, Szarvas T. Clinical sequencing identifies potential actionable alterations in a high rate of urachal and primary bladder adenocarcinomas. Cancer Med. 2023 Apr;12(7):9041-9054. doi: 10.1002/cam4.5639. **IF: 4.711**

12. Váradi M, Horváth O, Módos O, Fazekas T, Grunewald CM, Niegisch G, Krafft U, Grünwald V, Hadaschik B, Olah C, Maráz A, Furka A, Szűcs M, Nyirády P, Szarvas T. Efficacy of immune checkpoint inhibitor therapy for advanced urothelial carcinoma in real-life clinical practice: results of a multicentric, retrospective study. Sci Rep. 2023 Oct 13;13(1):17378. doi: 10.1038/s41598-023-44103-9. **IF: 4.6**

10. Acknowledgements

First, I would like to express my sincere gratitude to my supervisor, Prof. Dr. Tibor Szarvas, for his unwavering inspiration, guidance, and continuous support throughout the duration of the research project.

I am deeply appreciative of the Head of the Department of Urology at Semmelweis University, Prof. Dr. Péter Nyirády, and the Head of the Department of Urology at the University of Duisburg-Essen, Prof. Dr. Boris Hadaschik, for their instrumental roles in making this research possible. The collaboration between the two departments and the resources provided a solid foundation for this research project.

I would like to thank Dr. Henning Reis for his pivotal contributions and support in the immunobiological part of this research. His expertise and work had a crucial role in preparing this work and the papers related to it.

I would like to thank Dr. Fabian Mairinger for his invaluable assistance in conducting gene expression analysis using the NanoString method.

I would also like to extend my appreciation to all the members of the Uro-oncological research group at the Department of Urology, Semmelweis University, and my colleagues at the Research Laboratory, Experimental Urology at the University of Duisburg-Essen.

Finally, I am grateful to my parents, grandparents, and my entire family, who supported my education and research career. Their encouragement and belief in me have been a driving force behind my career, and I am truly thankful for their continuous support and love.